Brus group experimental areas

1. Carbon Nanotube Excited States:
Two photon study of Excitons
Rayleigh Scattering for identification of single tubes
Short tubes in the interstellar medium?

2. Transition metal oxide nanocrystals and nanowires:
electric force microscopy
hydrothermal and organometallic synthesis
structural phase transitions

3. Local electromagnetic field enhancement around Ag
Nanocrystals

Chemistry and Physics of Semiconductor Nanocrystals
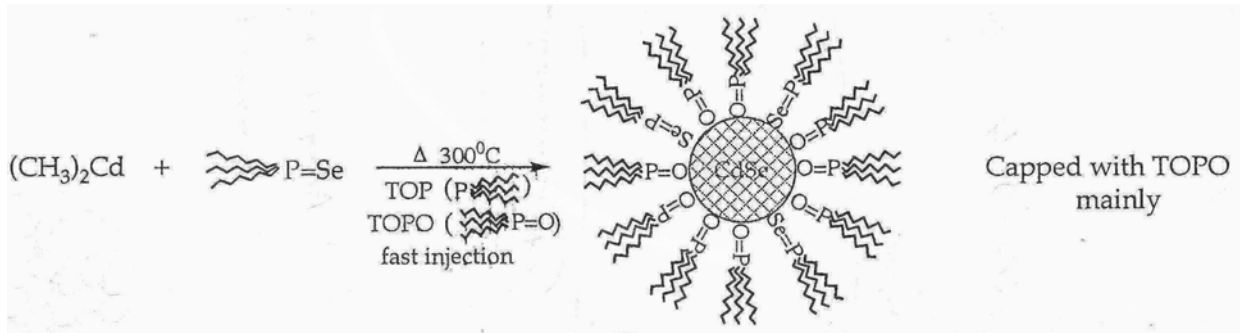
Louis Brus
Chemistry Department
Columbia University

History
Synthesis and self-assembly into solids
Electronic Structure and Luminescence
Optical Spectra of Single Nanocrystals
Charge State of Single Nanocrystals.

What is a CdSe nanocrystal?

$(CH_3)_2Cd$ + $\sim\sim\sim$P=Se $\xrightarrow[\substack{TOP\ (P\sim\sim\sim) \\ TOPO\ (\sim\sim\sim P=O) \\ \text{fast injection}}]{\Delta\ 300^0C}$ $\sim\sim\sim P=O$ (CdSe) O=P$\sim\sim\sim$ Capped with TOPO mainly

- Organic molecules 'cap' the outer surface of core semiconductor. They prevent aggregation, oxidation, and stabilize nanoparticles in the solution. Most important, they electronically isolate the particles and passivate the surface states.

Xiaogang Peng
Arkansas

CdSe

% Surface atoms vs **Diameter (nm)** — **Chemical Potential**
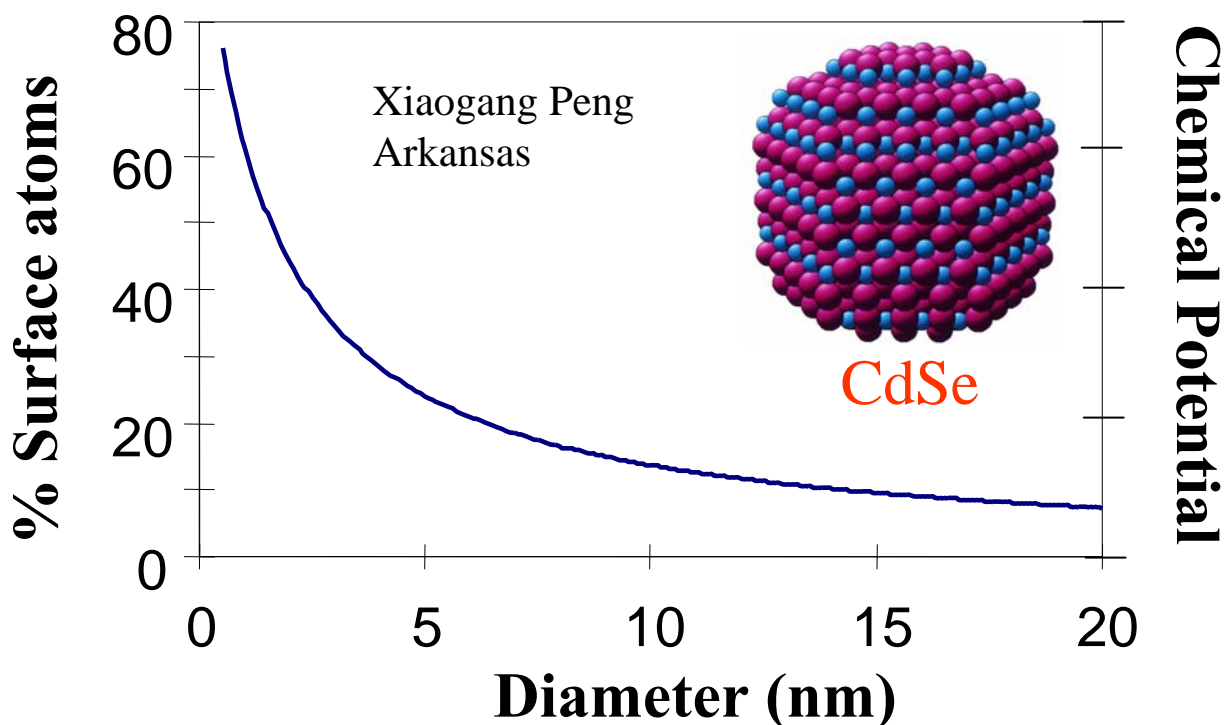
1983

Quantum size effects in the redox potentials, resonance Raman spectra, and electronic spectra of CdS crystallites in aqueous solution

R. Rossetti, S. Nakahara, and L. E. Brus

Bell Laboratories, Murray Hill, New Jersey 07974

We report observation of size effects in the excited electronic properties of small, crystalline CdS particles. We also theoretically model the leading small size correction terms applicable to the photochemical redox potentials and lowest exciton energy. Our experiment involves controlled formation of CdS crystallites in aqueous solution; the photophysics and surface redox chemistry of electrons e^- and holes h^+ in these colloidal crystallites has been of recent interest.[1–6]

Transmission electron microscope examination of particles from a freshly prepared colloid shows a narrow size distribution.[7] A typical particle diameter is $\simeq 35$ Å, which corresponds to about six unit cells. The mass weighted average diameter $\bar{d}$ is $\simeq 45$ Å. The particles are crystalline (cubic CdS), with moderate diffraction ring broadening due to small crystallite size. In colloidal solution, thermodynamics favors growth of larger crystallites at the expense of smaller ones. We observe that, if these colloids "age" for $\simeq 1$ day at pH 3, the size distribution becomes broader with $\bar{d} \simeq 125$ Å. On the average, 21 small crystallites dissolve and recrystallize onto one larger "seed" crystallite. The colloid remains transparent without CdS precipitation as it ages. The crystal structure is mixed cubic and hexagonal after aging; the hexagonal phase is thermodynamically more stable.

Resonance Raman (RR) spectroscopy[8] in principle allows an *in situ* vibrational characterization despite the low crystallite concentration $\simeq 2 \times 10^{-6}$ M in fresh colloids. The 416 nm RR spectrum in Fig. 1 shows the LO (longitudinal optical) phonon at 305 cm^{-1} and a weaker overtone near 605 cm^{-1}. These CdS peaks are superimposed on nearly continuous water Raman scattering. $e^- - h^+$ recombination luminescence has been largely quenched by addition of $\simeq 10^{-3}$ M benzoquinone.[3] At 395, 448, and 460 nm similar spectra are observed. To the red (480, 503, and 532 nm) and to the blue (355 and 266 nm), the CdS RR spectra are far weaker and not detected.

To our knowledge these are the smallest isolated crystallites that have been examined by Raman spectroscopy.[9,10] The LO peak occurs within a couple of cm^{-1} of the bulk CdS frequency. In Fig. 1 the low frequency wing, in the region of expected surface mode maxima,[11] is slightly stronger than the high frequency wing. In other fresh colloids, the LO peak is more symmetrical. Shifts and surface mode maxima have been reported for small crystalline grains in Si films.[12,13]

In aged colloids the CdS RR excitation spectrum changes markedly. RR scattering at 395, 416, and 448 nm is not detectable, with the cross section per unit mass decreasing by at least a factor of 10. Recall that there is no loss of CdS mass during aging; mass shifts from smaller to larger crystallites. CdS RR scattering is detected in the red shifted and narrower spectral range 463–480 nm. The spectra are similar to those in Fig. 1, with an LO peak decrease of $\simeq 3$ cm^{-1} and a slight narrowing.

Letters to the Editor
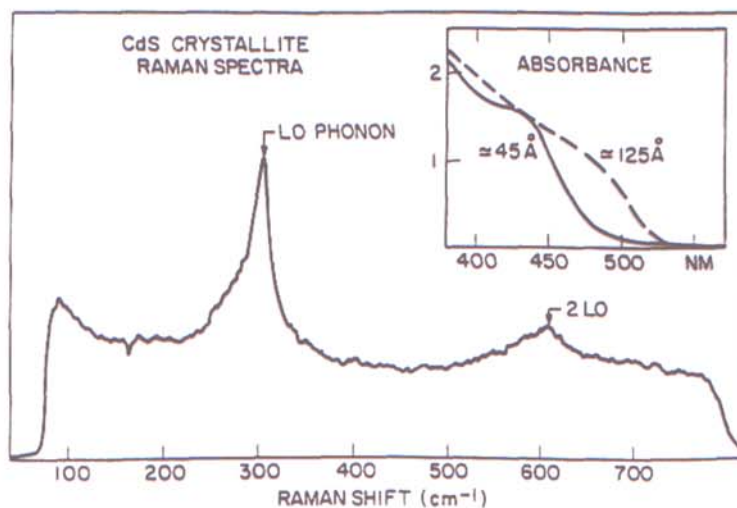
Organometallic synthesis, controlled Growth, Surface "capping"

and isolation of stabilized clusters

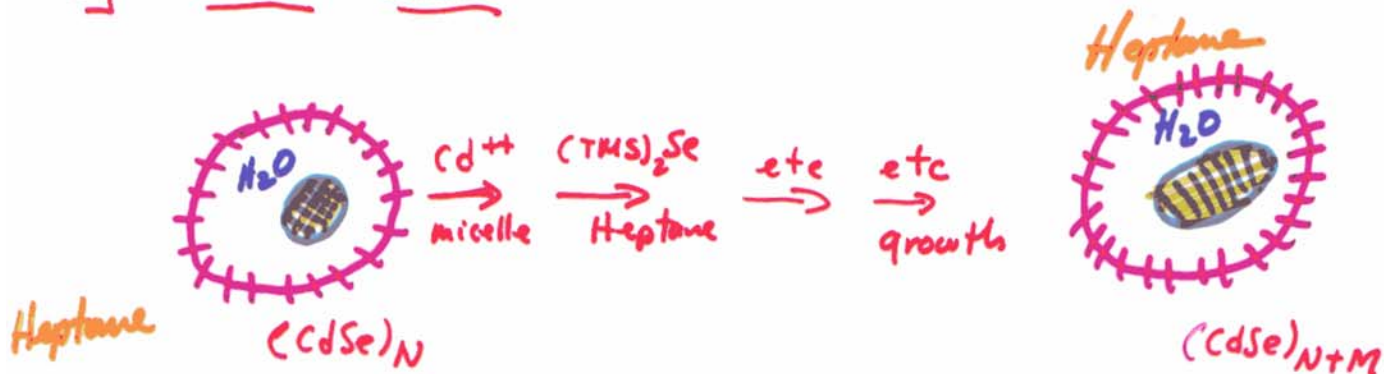A] Take advantage of hydrocarbon
phase — hydrophobic reagents

✱ Mike Steigerwald
Paul Alivisatos
Lou Brus

Cd^+ H_2O Heptane $+ (Me_3Si)_2Se$ in Heptane $\xrightarrow{growth}$ H_2O $(CdSe)_N$ crystallite Heptane

small	18 Å	$N \simeq 70$
large	50 Å	$N \simeq 630$
standard deviation 20%		

dry → redissolve → heptane colloid

B] Controlled Growth

$(CdSe)_N$ Heptane H_2O $\xrightarrow[micelle]{Cd^{++}}$ $\xrightarrow{(TMS)_2Se}$ $\xrightarrow{etc}$ $\xrightarrow[growth]{etc}$ H_2O Heptane $(CdSe)_{N+M}$
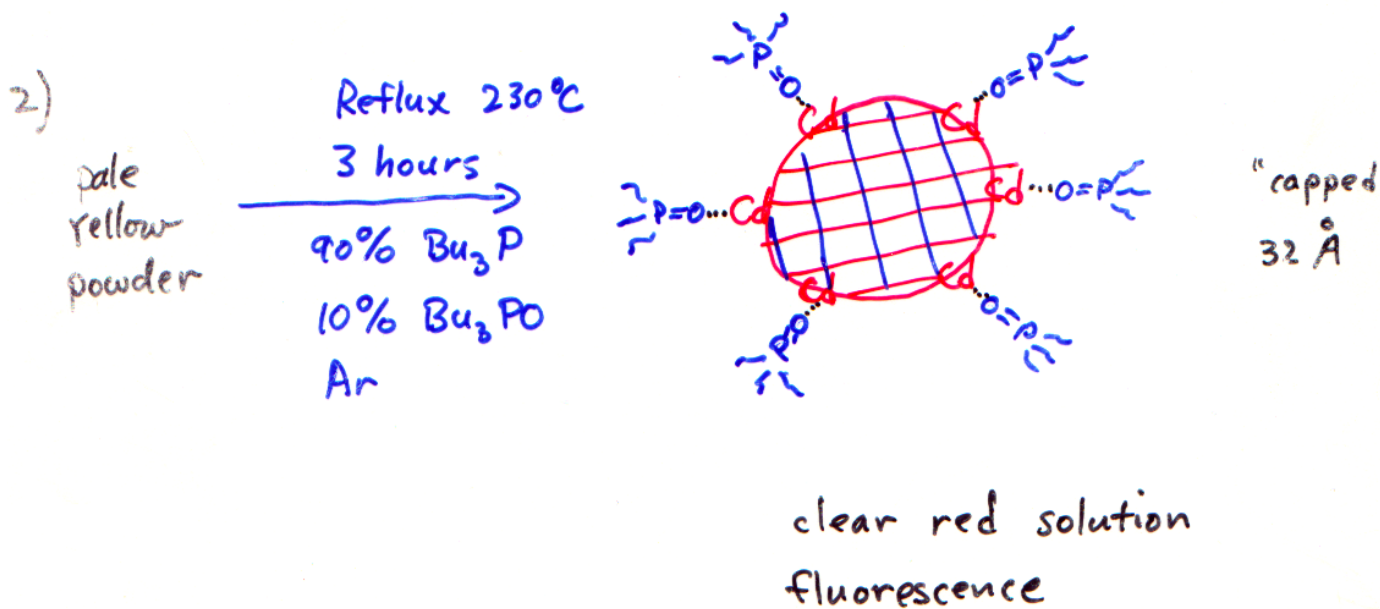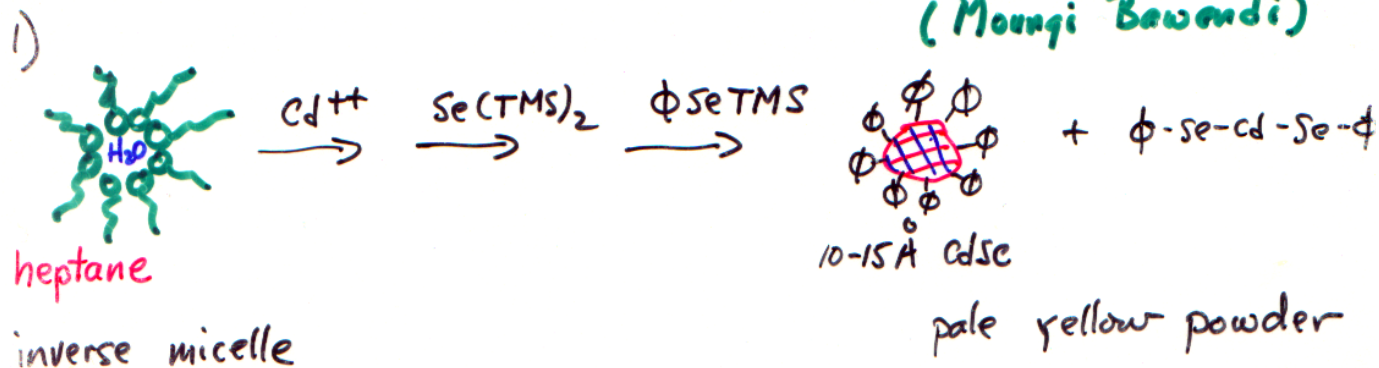
Crystallite in micelle, with water present,
is stable yet can grow further
⟹ exotic chemistry on surface
⟹ concentric growth of one material on
another

Synthesis 1988   Bawendi etal J. Chem. Phys. 91, 7282 (1989)

Two Step Organometallic Synthesis of CdSe Single Crystallites
(Mike Steigerwald)
(Moungi Bawendi)

1)

heptane

inverse micelle

$Cd^{++} \xrightarrow{} Se(TMS)_2 \xrightarrow{} \phi SeTMS \xrightarrow{}$ + ϕ-Se-Cd-Se-ϕ

10-15 Å CdSe

pale yellow powder

2)

pale
yellow
powder

Reflux 230°C
3 hours
$\xrightarrow{}$
90% Bu_3P
10% Bu_3PO
Ar

"capped
32 Å

clear red solution
fluorescence

Characterization

TEM   Pat Carroll
Powder x-ray   Refik Korten
^{77}Se NMR   Peter Reynders
Se, Cd EXAFS   Matt Marcus

Chemical synthesis of CdSe nanocrystals

Thermocouple

Argon gas at little above ambient pressure

- Narrow size distribution (~5%) is obtained by the fast injection of the chemical reagents into the flask at high temperature (~ 350 ^{0}C).

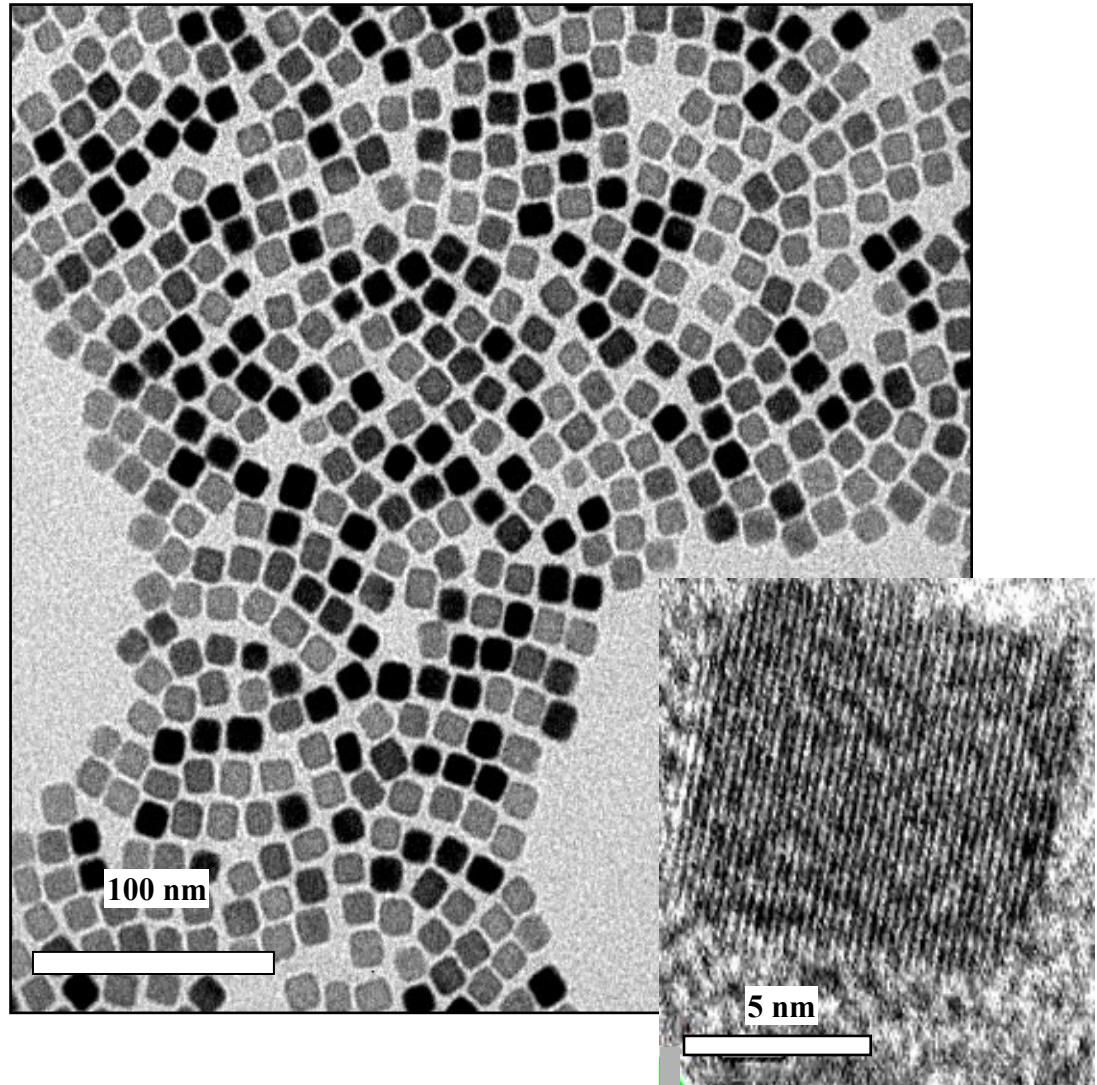- The precursors are prepared in the glove box to avoid oxygen and water.

Semiconductor: CdSe, CdTe, PbSe, etc.
Metal: PtFe

TEM of cubic PbSe nanocrystals

100 nm

5 nm

TEM images of PbSe quantum cubes after size selection (reaction temperature 215ºC), size ~12 nm

Change of shape from spheric to cubic in the size regime of 8 to 11 nm

Chris Murray, Wolfgang Gaschler, Franz Redl, IBM-Columbia

Low Temperature oganometallic Synthesis of TiO$_2$

$$Ti + OS(CH_3)_2$$

23 C   OPR$_3$ ligand

120°C

OPR$_3$ ligand
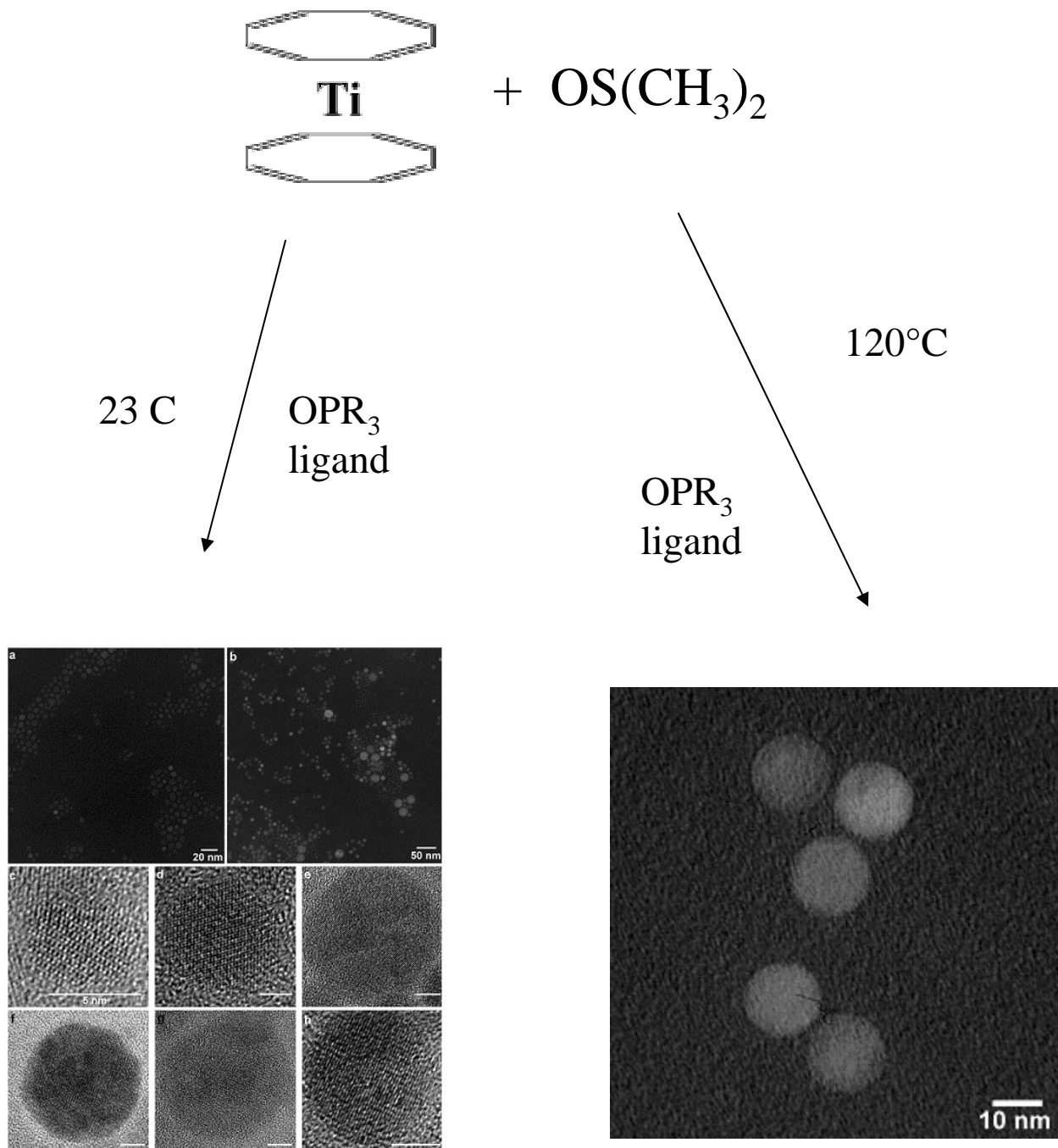
Jing Tang, Franz Redl, Yimei Zhu, Theo Siegrist, Louis E. Brus and Michael L. Steigerwald, "A Low-Temperature Synthesis of TiO2 Nanoparticles" , Nano Letters **5**, 543-548 (2005).
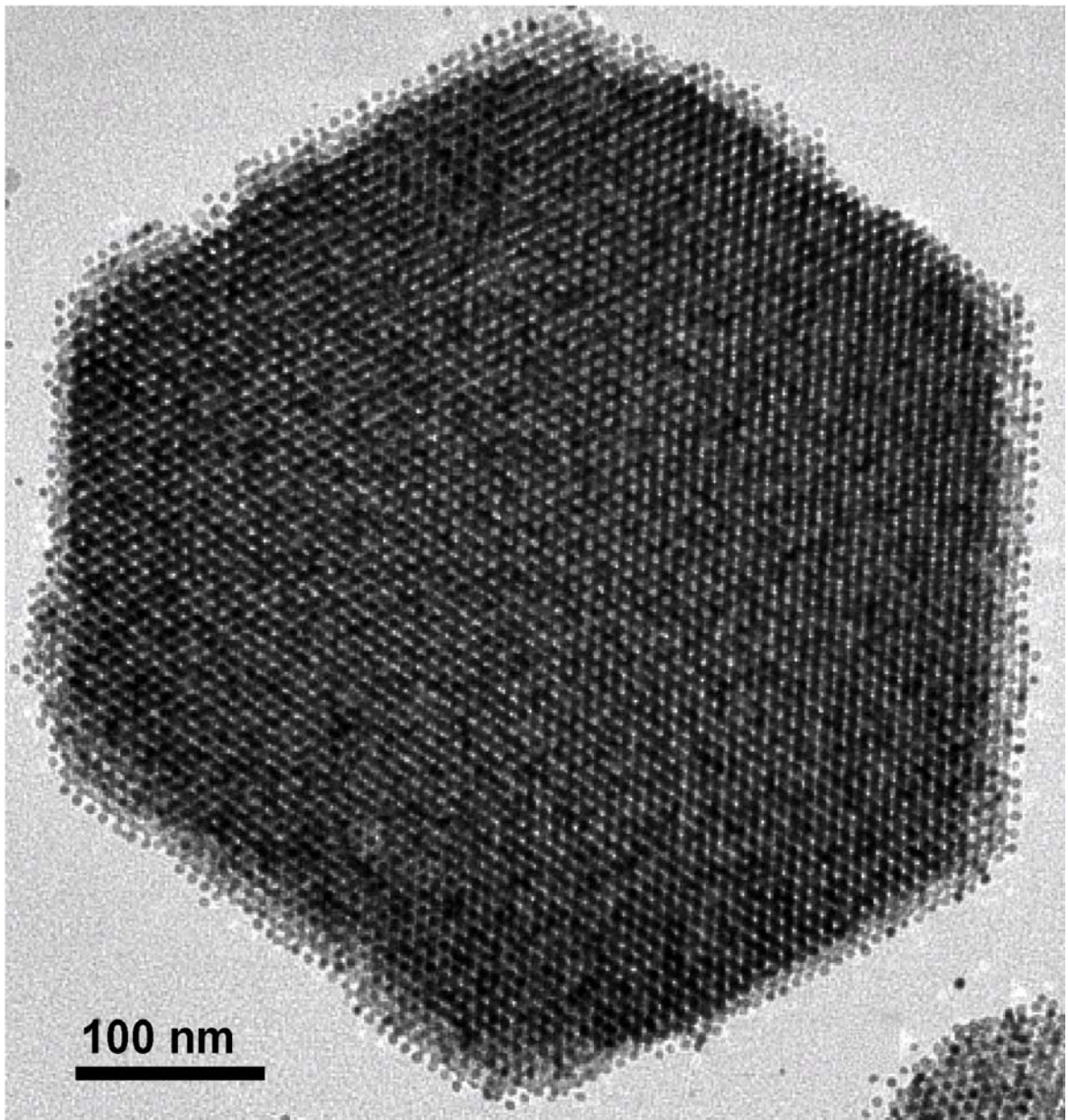
Growth of wires and exotic shapes
With junctions between different materials
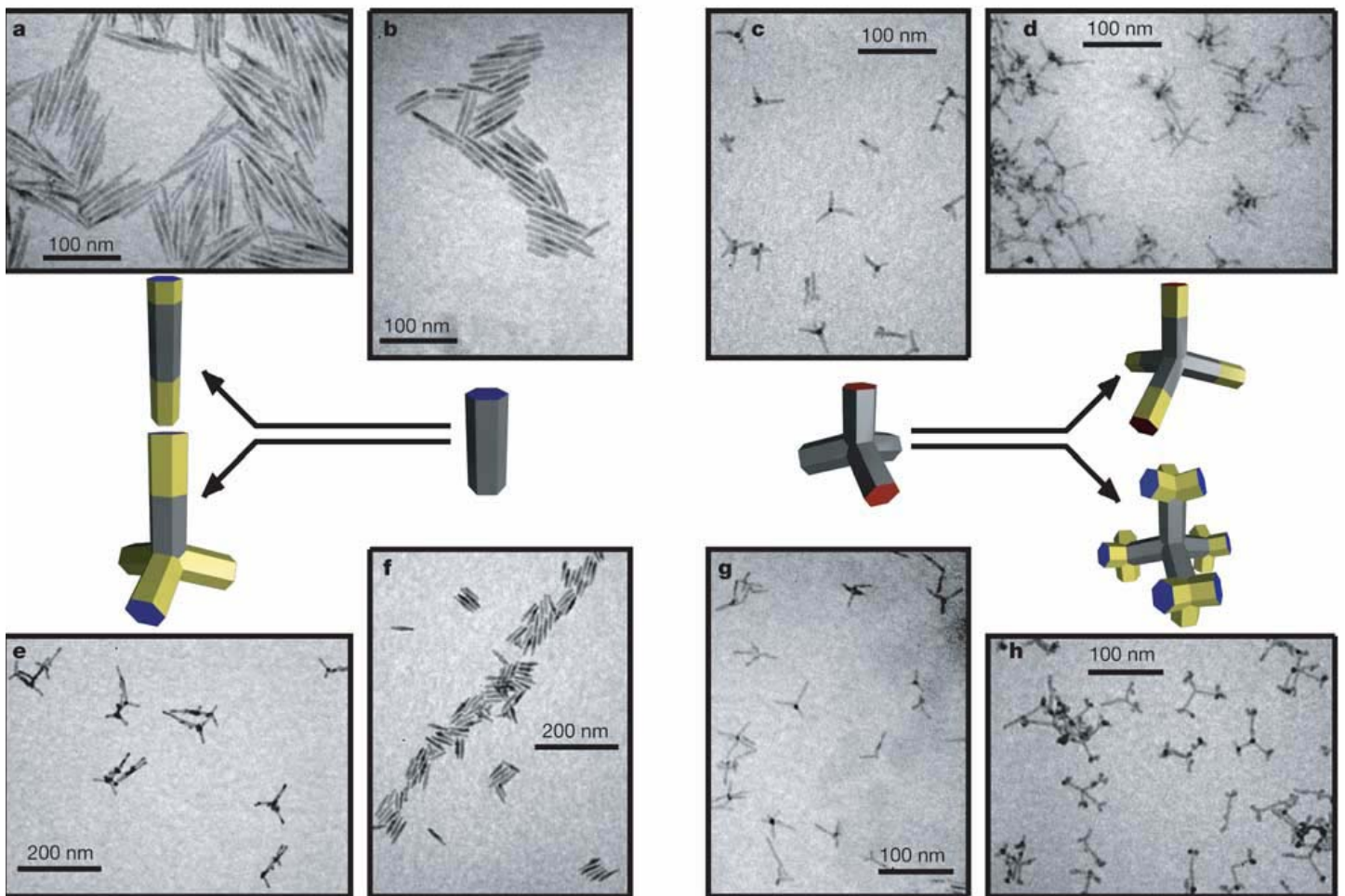
3D solid structures

Elena Shevchenko
O'Brien – Murray
Columbia-IBM

CoPt$_3$ nanoparticles

Bimodal superlattice of 11 nm magnetic Fe_2O_3 NCs and semiconducting 5 nm PbSe NCs
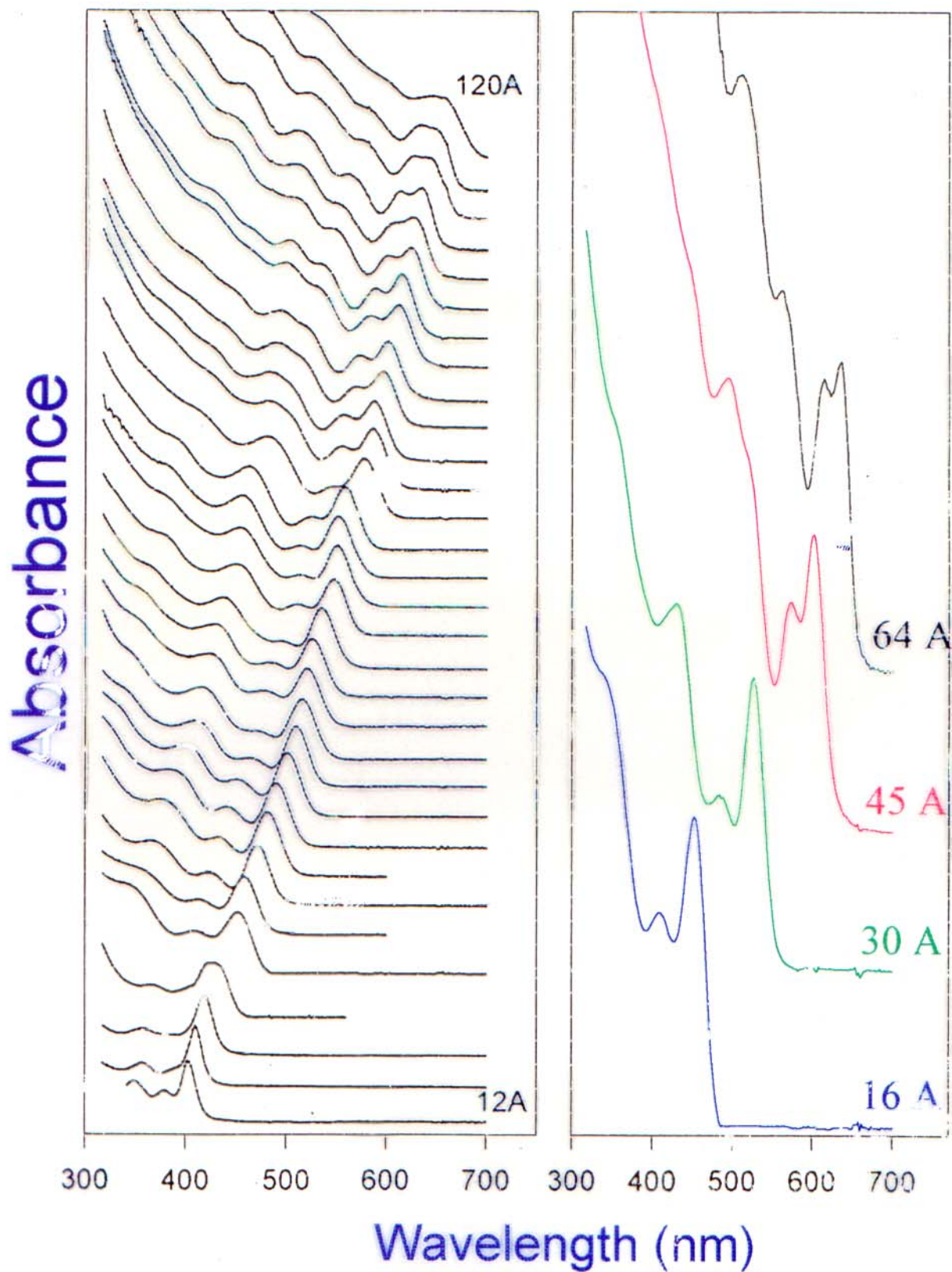
Redl, Cho, Murray, O'Brien Nature 423, 968 (2003)
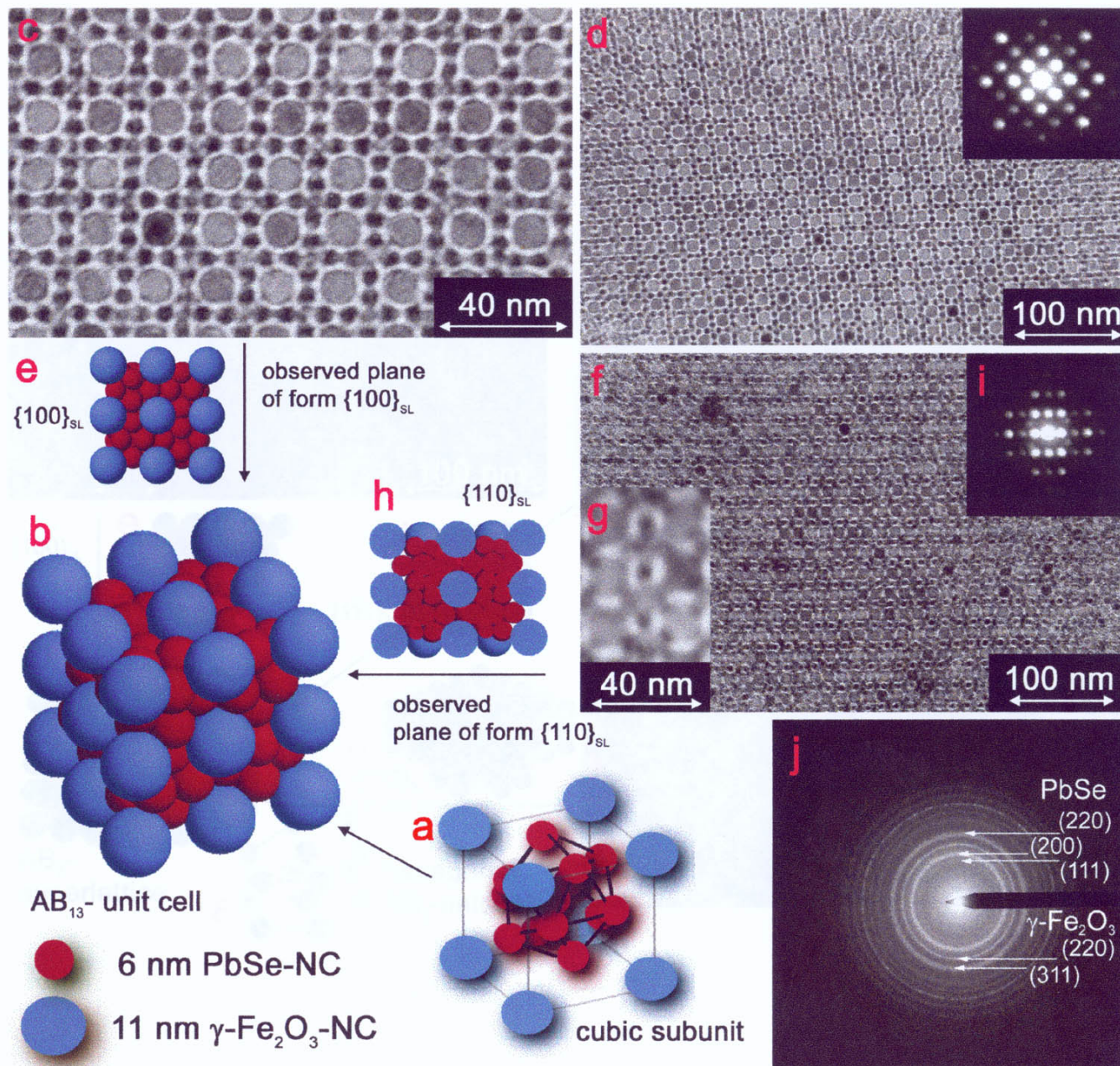
CdSe Size Dependent Absorbance

C. Murray and M. Bawendi
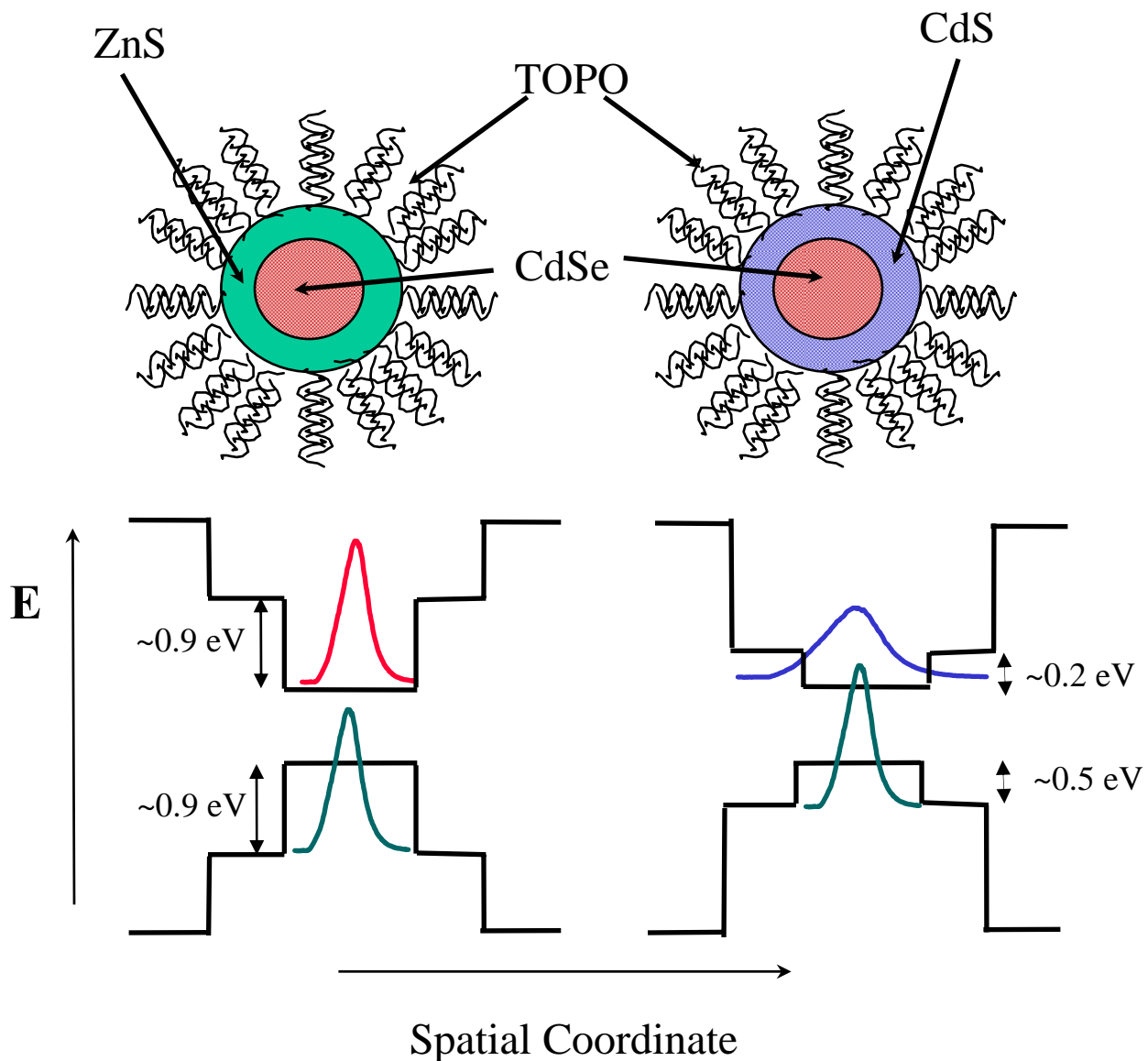
Chris Murray & Moungi Bawendi (MIT)

Size tunable luminescence
Narrow emission band

High Quantum Yield Luminescence
More stable than dye molecules
Possible use in biological imaging

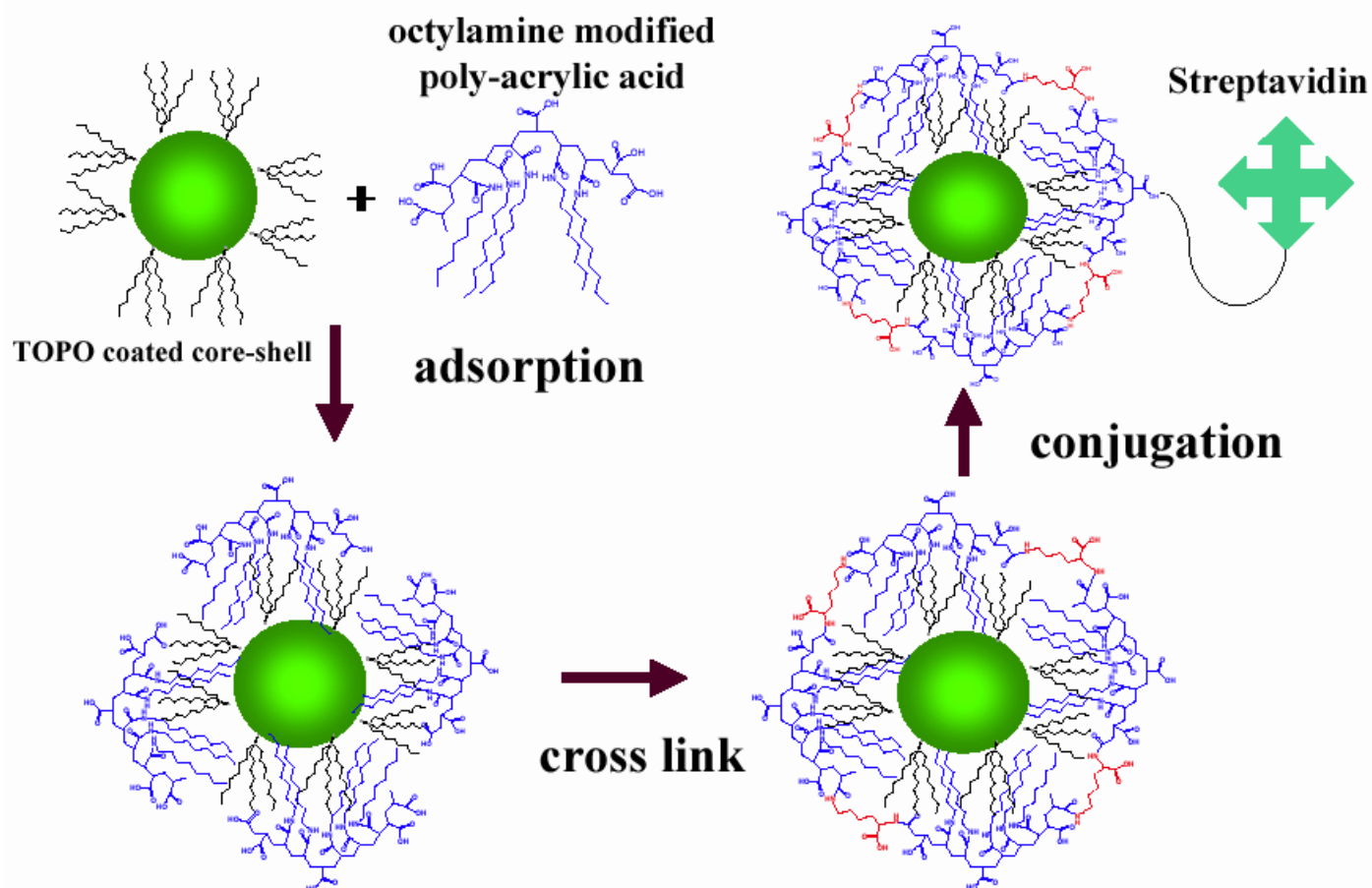# ZnS surface shell layer "insulates" the luminescent CdSe core

high quantum yield and photostability

B. O. Dabbousi, *et al.* (1997)
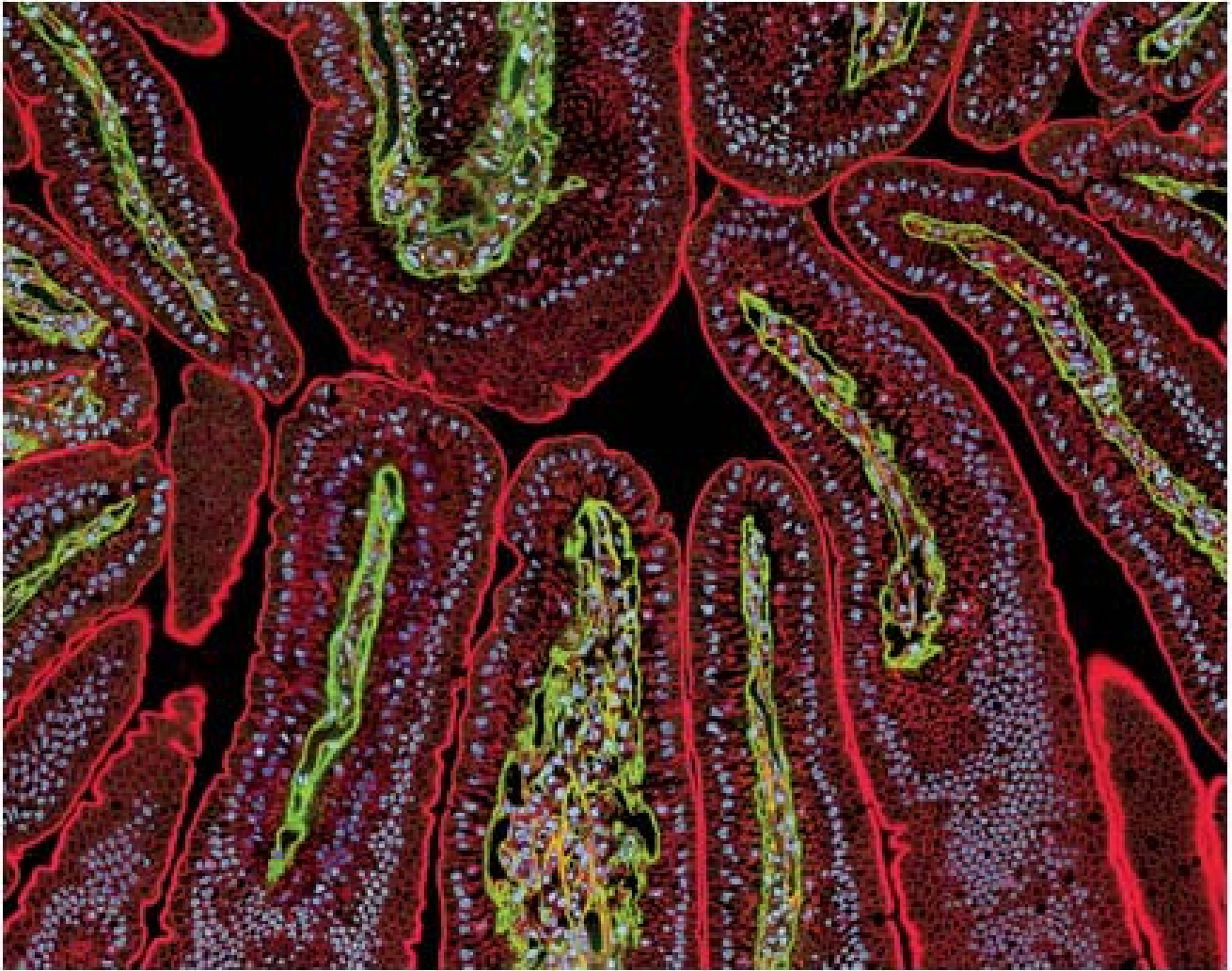
Biological Imaging Applications

Surface Stabilization & Biomolecule Conjugation

octylamine modified poly-acrylic acid

TOPO coated core-shell

adsorption

cross link

conjugation

Streptavidin

Q Dot Corporation
www.qdots.com

Published in Nature Biotechnology Online

Imaging Mouse Intestine

A mouse intestinal section visualized using fluorescent Qdot nanocrystal conjugates. Actin was labeled with a mouse anti-actin monoclonal antibody and visualized using red-fluorescent Qdot 655 goat F(ab')2 anti–mouse IgG (Q11022MP, Q11221MP). Laminin was labeled with a rabbit anti-laminin polyclonal antibody and visualized using green-fluorescent Qdot 525 goat F(ab')2 anti–rabbit IgG (Q11441MP). Nuclei were stained with blue-fluorescent Hoechst 33342 (H1399, H3570, H21492). Image contributed by Thomas Deerinck and Mark Ellisman, The National Center for Microscopy and Imaging Research, San Diego,
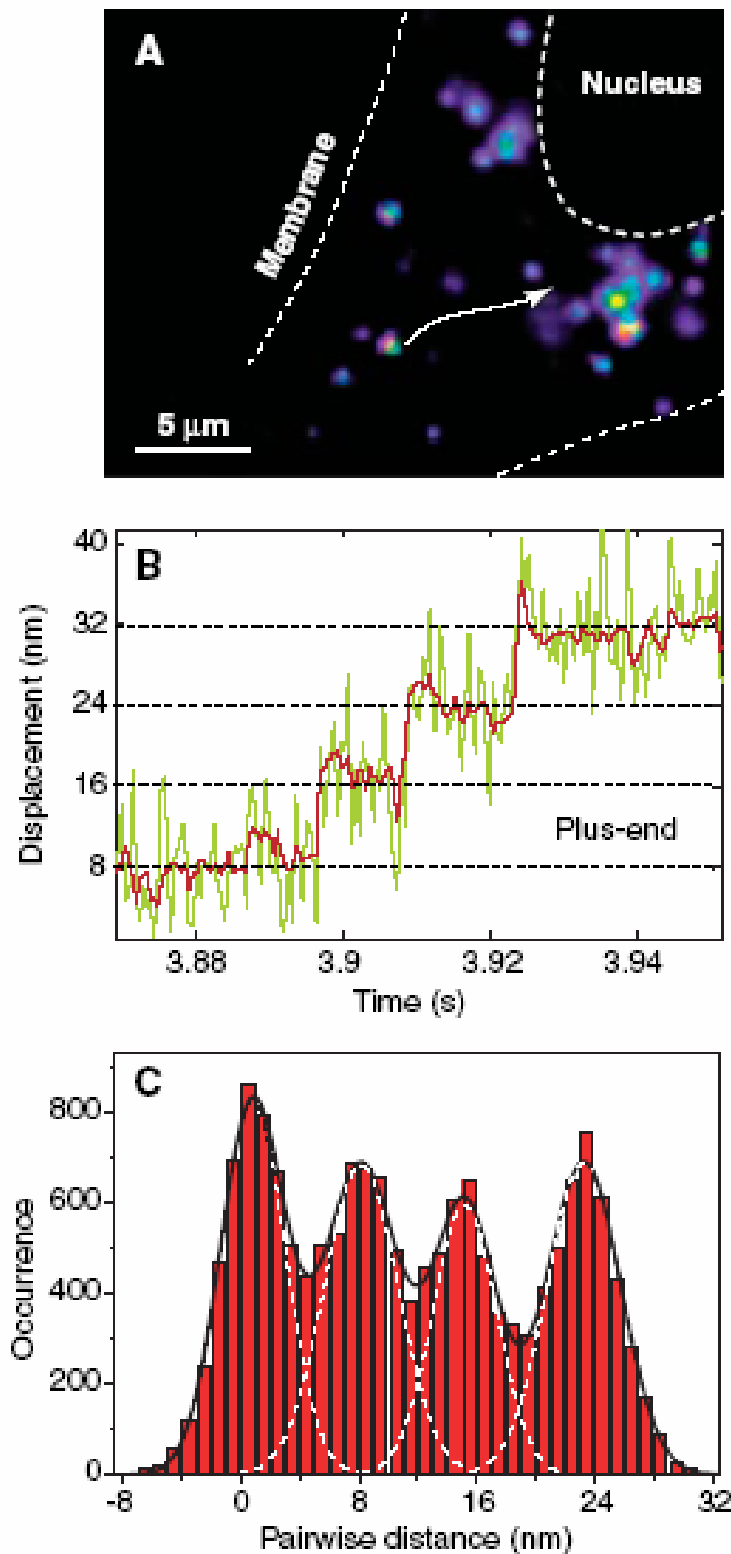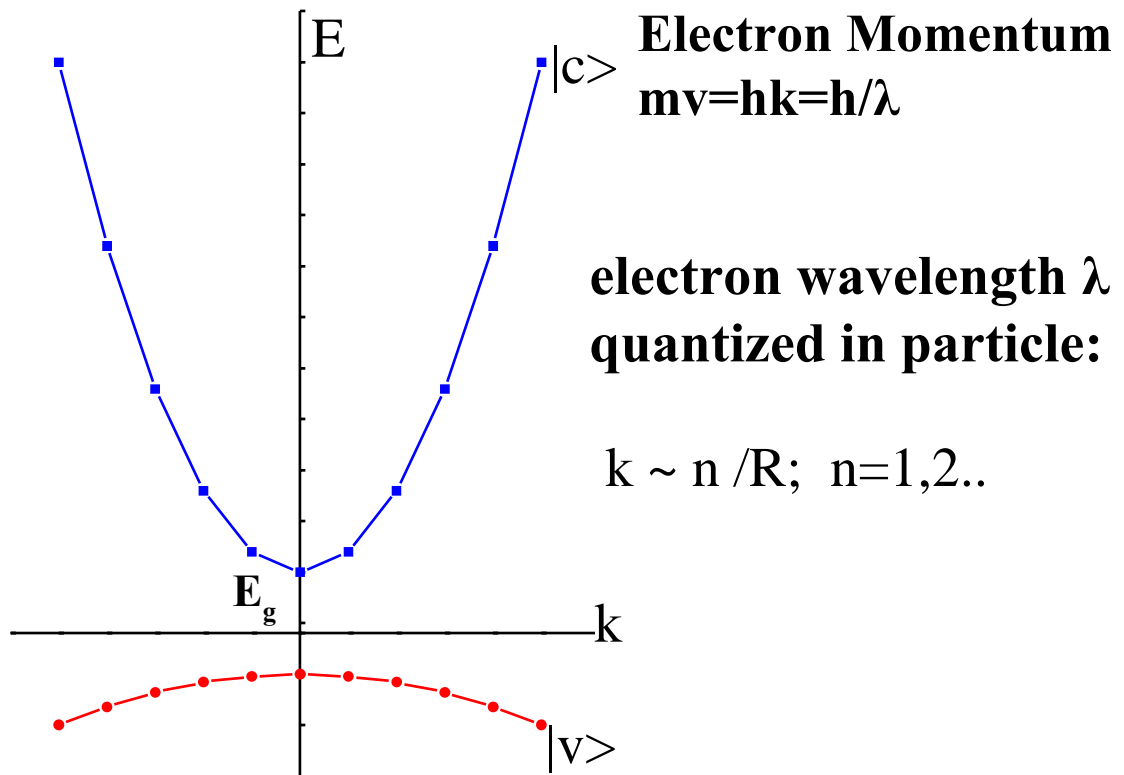
Kinetics of Microtubule Motor Steps

Fig. 2. Observation of individual microtubule motor steps in a live cell with endocytosed quantum dots. (**A**) Live A549 cell with QD-containing endosomes (bright dots), many of which undergo active transport by kinesin (outward movements) or dynein (inward movements, white arrow). (**B**) Displacement trajectory of a outward-going (microtubule plus-end) endosome, exhibiting stepwise movements of the underlying motor (likely kinesin). Green, raw data; red, filtered data. (**C**) Pairwise distance histogram of the filtered displacement trace in (B), with an 8-nm spacing between adjacent peaks.

Sunney Xie etal, Science 312, 228 (2006)

Simple Model for Electronic Structure:
Quantum Size Effect

Electron Momentum
$mv = hk = h/\lambda$

electron wavelength λ
quantized in particle:

$k \sim n/R; \quad n = 1, 2..$

• Energy of HOMO-LUMO Blue Shifted from bulk band gap

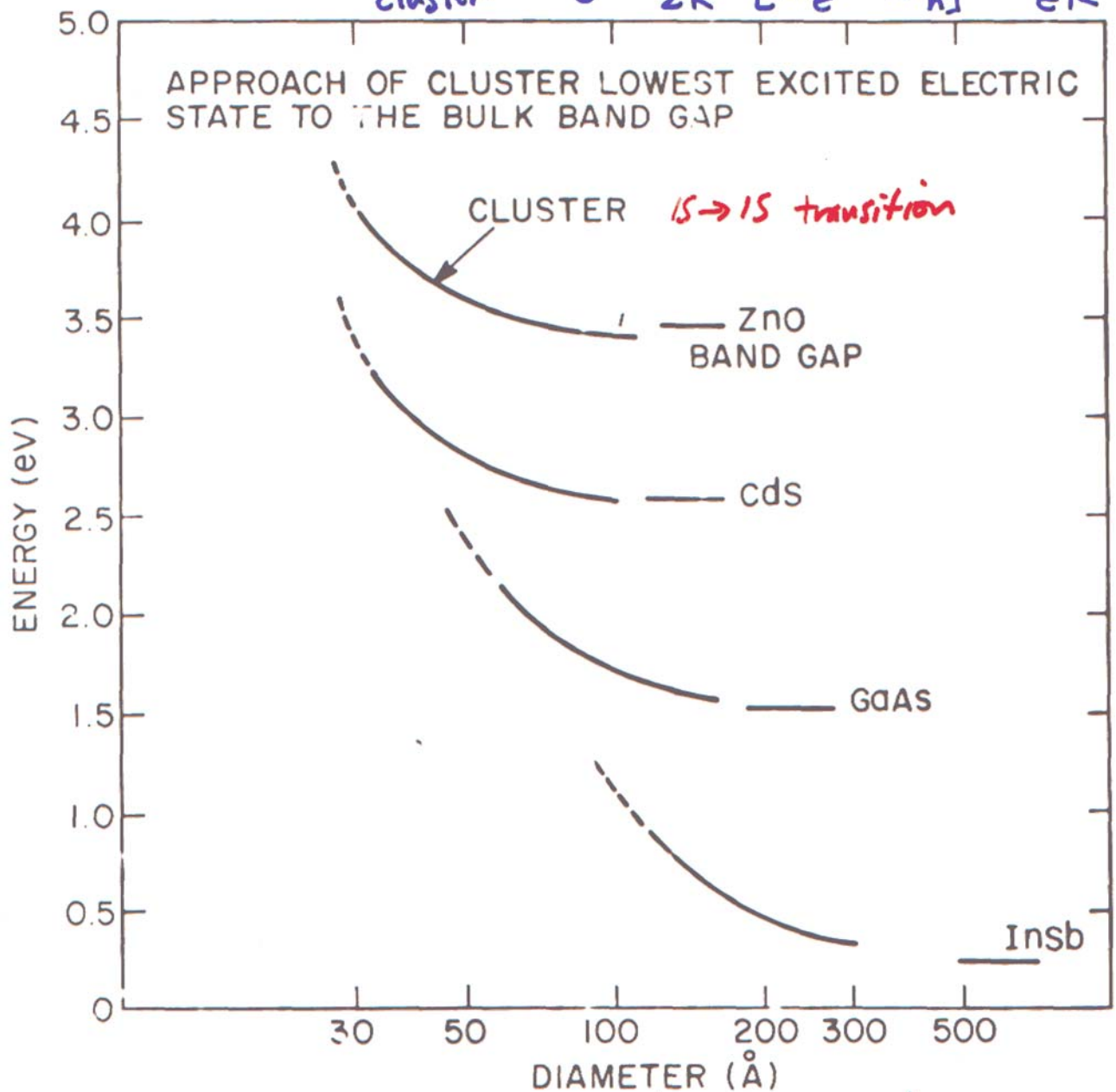$$E(k) \sim E_g + n^2 h^2/(8m_e R^2) + n^2 h^2/(8m_h R^2)$$

• Optical Spectra are Discrete and Size Dependent

• Model uses known bulk band structure, and ignores
• bonding reconstruction on surfaces

Quantum Size Effect including Electrostatics

Electron Correlation — Coulomb attraction between e^- and h^+

$$\Psi \simeq \phi_{1S}(r_e)\,\phi_{1S}(r_h) \qquad \text{zero order}$$

$$E^*_{cluster} = E_g + \frac{\hbar^2\pi^2}{2R^2}\left[\frac{1}{m_e} + \frac{1}{m_h}\right] - \frac{1.8e^2}{\epsilon R} +$$

APPROACH OF CLUSTER LOWEST EXCITED ELECTRIC
STATE TO THE BULK BAND GAP

CLUSTER $1S \rightarrow 1S$ transition

— ZnO
BAND GAP

— CdS

— GaAs

— InSb

ENERGY (eV)

DIAMETER (Å)

No adjustable parameters!

L. Brus, J. Chem. Phys. 79, 5566 (1983); 80, 4403 (1983)

Failure of Quantum Model in Silicon Nanocrystals:

Why does an H passivated 1.3 nm silicon nanocrystal emit in the blue, but an 1.3 nm oxide shell passivated nanocrystal emit in the red?
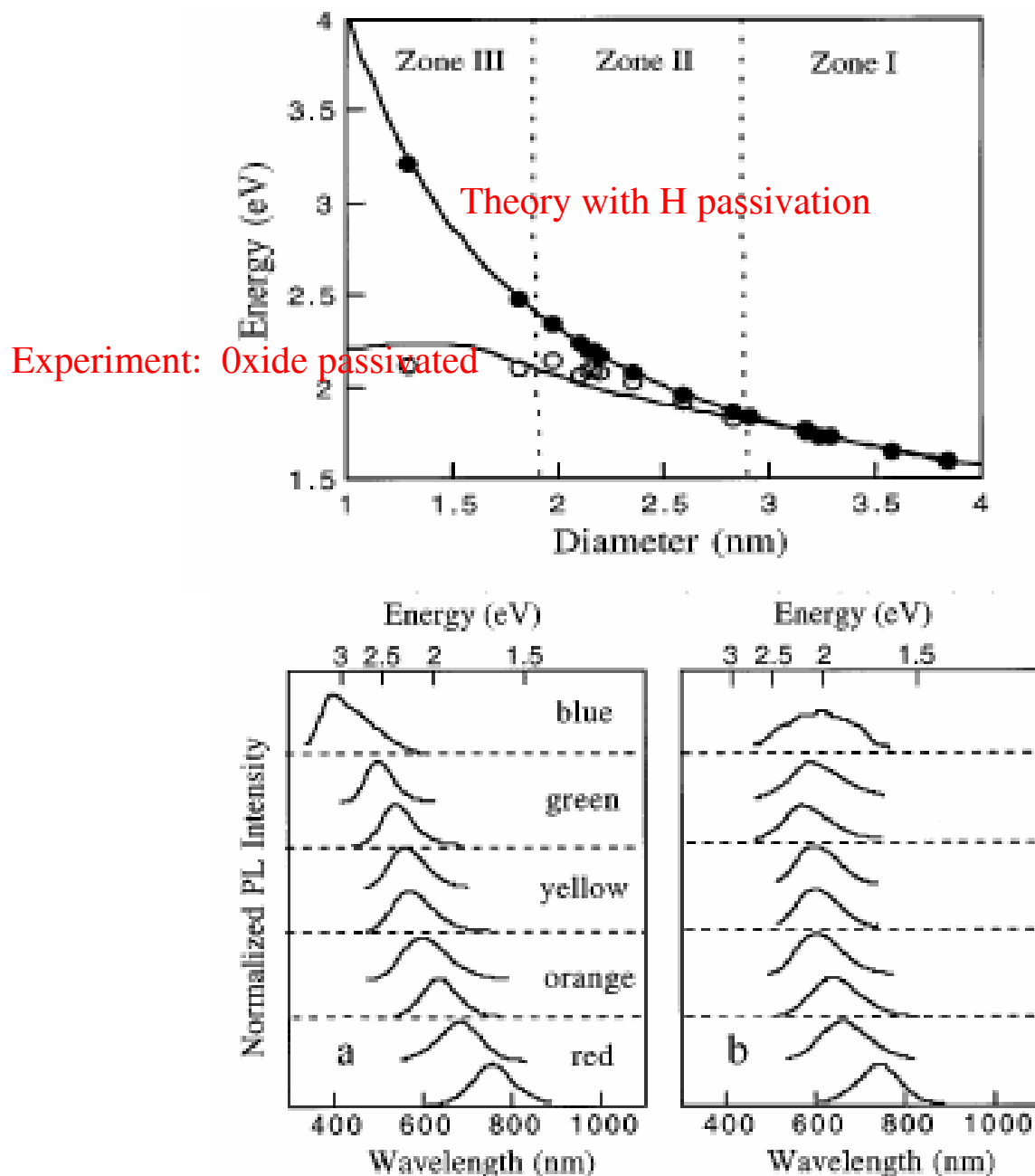

FIG. 1. Room temperature photoluminescence spectra from PSi samples with different porosities kept under Ar atmosphere (a) and after exposure to air (b).

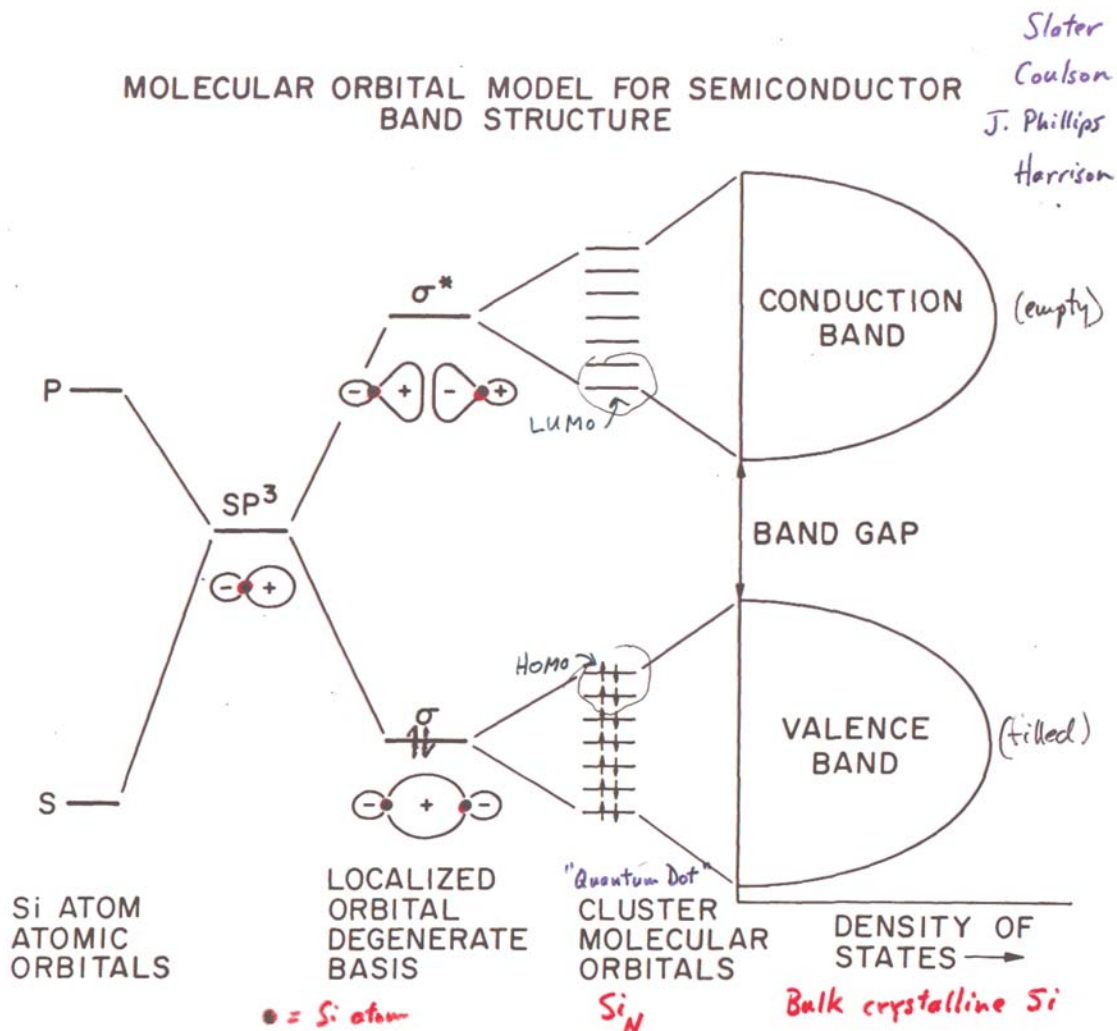Wolkin etal Phys Rev Lett 82, 197 (1999)

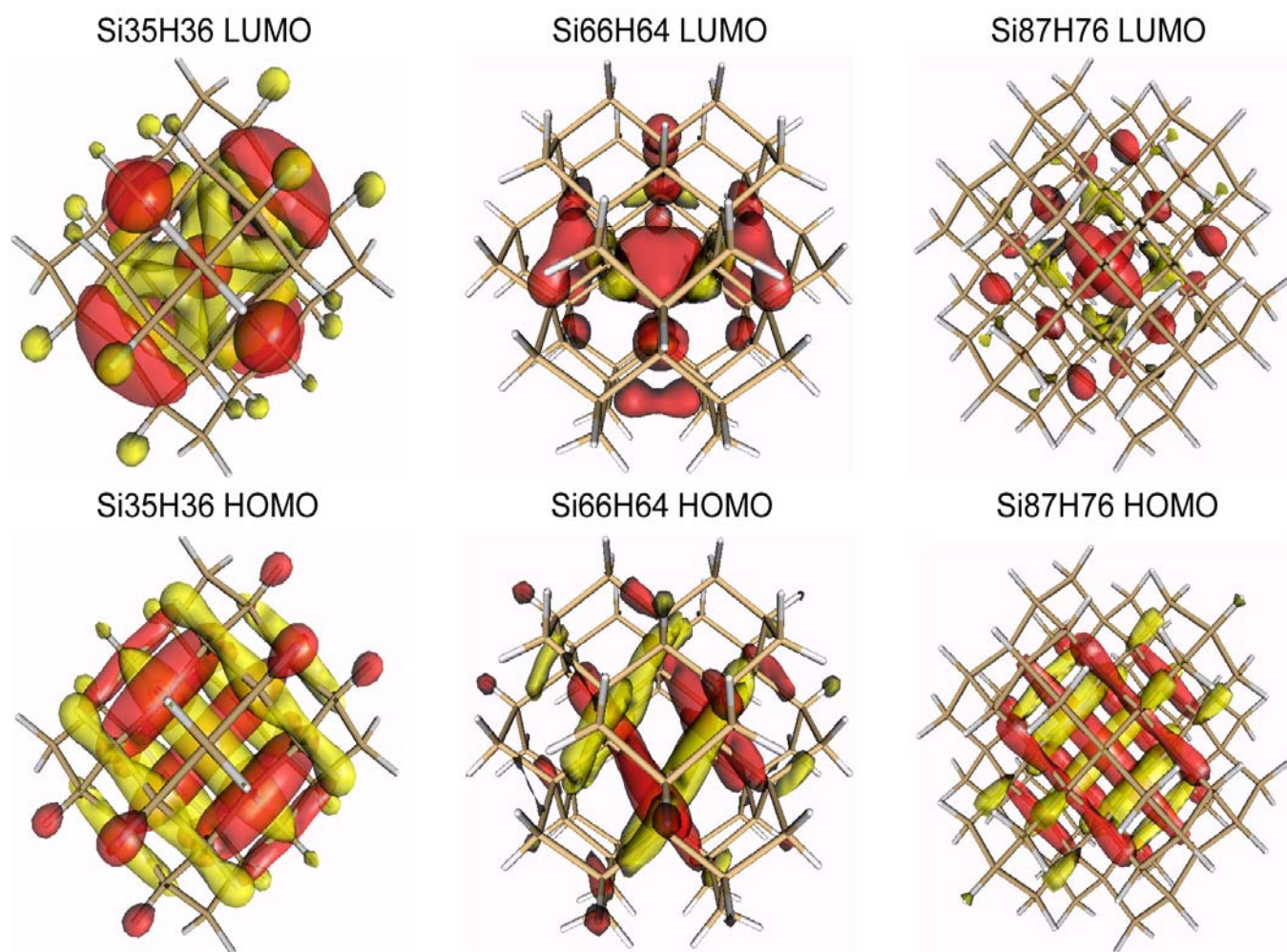# Ab Initio Electronic Structure Calculation

Surface Bonding and Geometrical Optimization
Independent of bulk band structure
Molecular Orbitals extend over entire nanocrystal

Problem: too many atoms

MOLECULAR ORBITAL MODEL FOR SEMICONDUCTOR BAND STRUCTURE

HOMO & LUMO of H-passivated Nanocrystals

Si35H36 LUMO   Si66H64 LUMO   Si87H76 LUMO

Si35H36 HOMO   Si66H64 HOMO   Si87H76 HOMO

As sizes increases, a 1S orbital with nodes on the surface is formed - expected behavior

Zhou, Friesner, Brus Nanoletters **3**, 163 (2003)
JACS **125**, 15599 (2003)
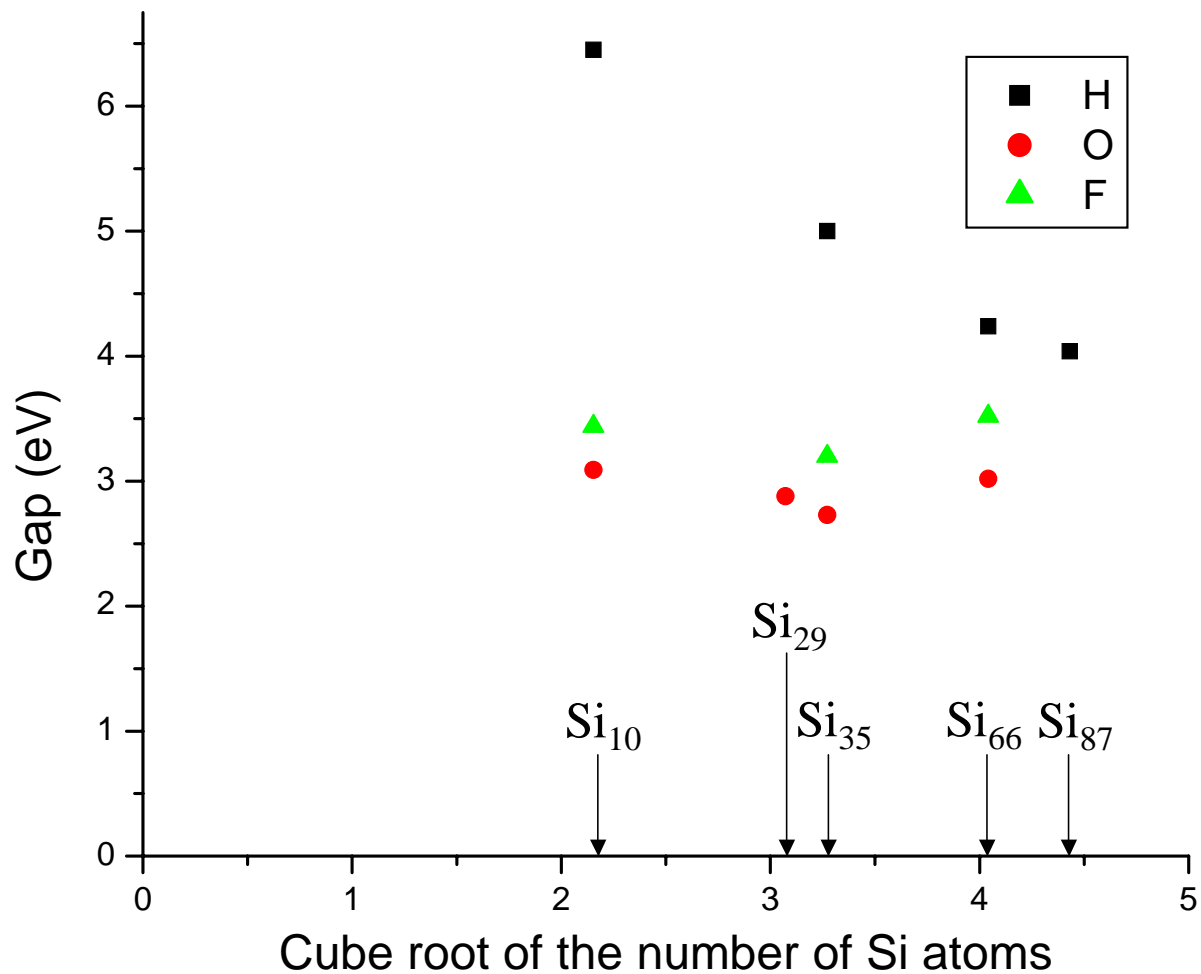
Molecular Orbitals of Si66 Species

158 atoms, 468 normal modes, 1380 electrons
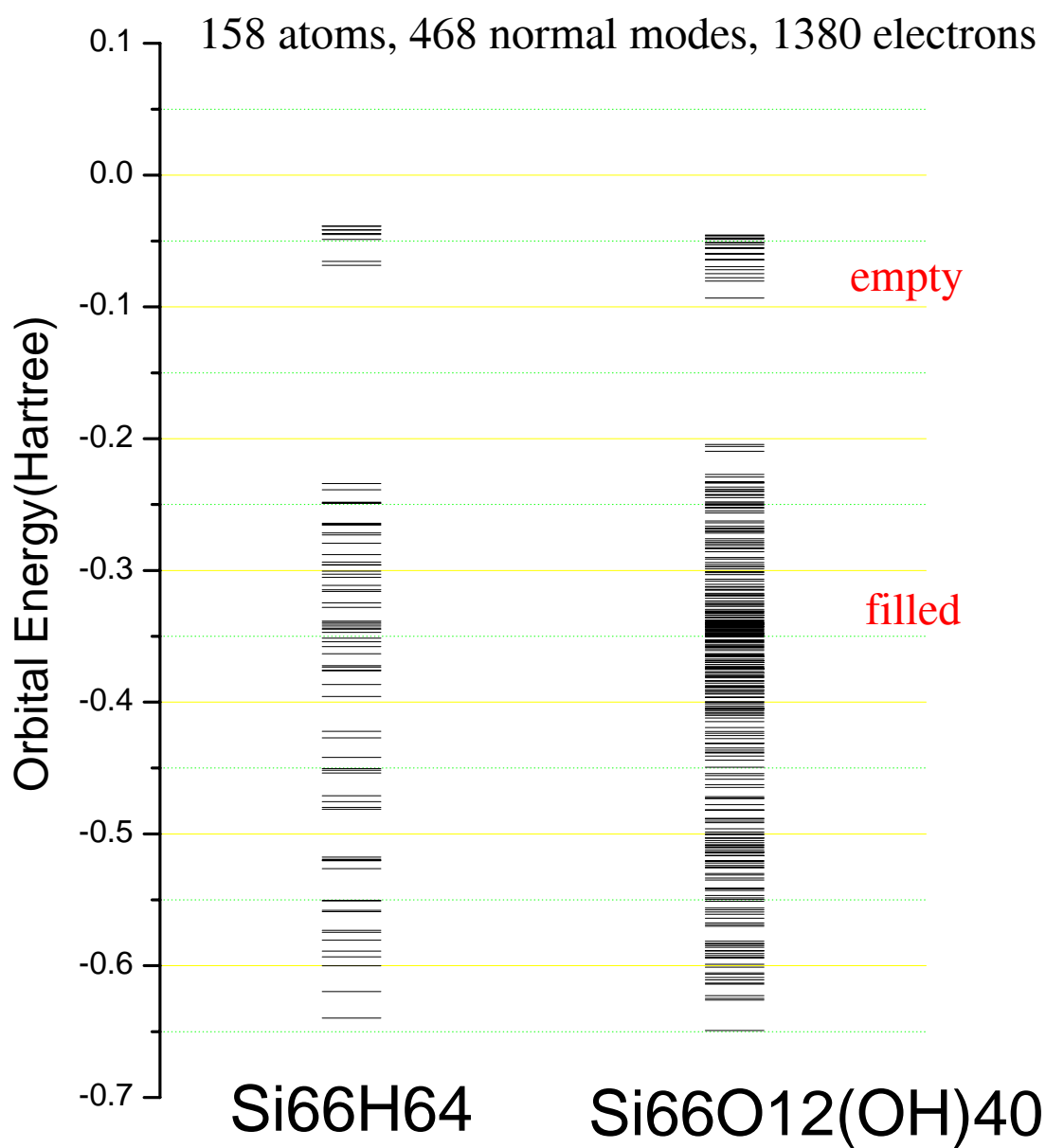
Oxide passivation lowers band gap by 1.5 eV
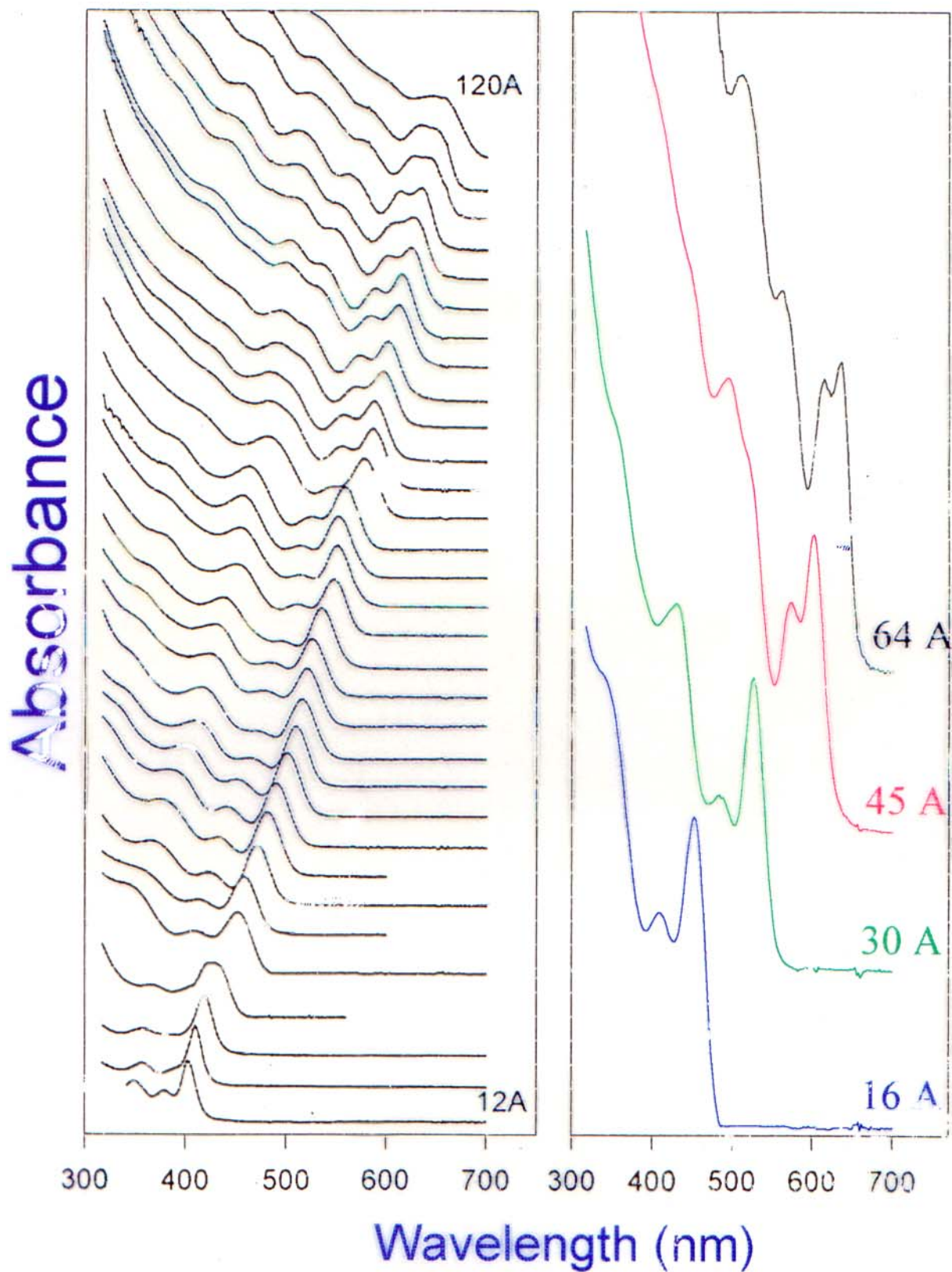LUMO moves down
HOMO moves up

Fermi level unchanged; hardness decreases

Si Nanocrystal Band Gap
Depends Upon Surface Passivation

Quantum size effect model works well when
 electronegativity of capping atom matches that
of lattice atom.

CdSe Size Dependent Absorbance

Absorbance

120A

12A

64 A

45 A

30 A

16 A

Wavelength (nm)

300 400 500 600 700

Bawendi group

Chris Murray & Moungi Bawendi (MIT)

How can we observe the band gap luminescence
 of single nanocrystals?

Nanocrystals have several thousand atoms
Size distribution ca. 5% in diameter
Each nanocrystal is unique
Spectra average over distributions

Experimental Setup: Far-Field Illumination
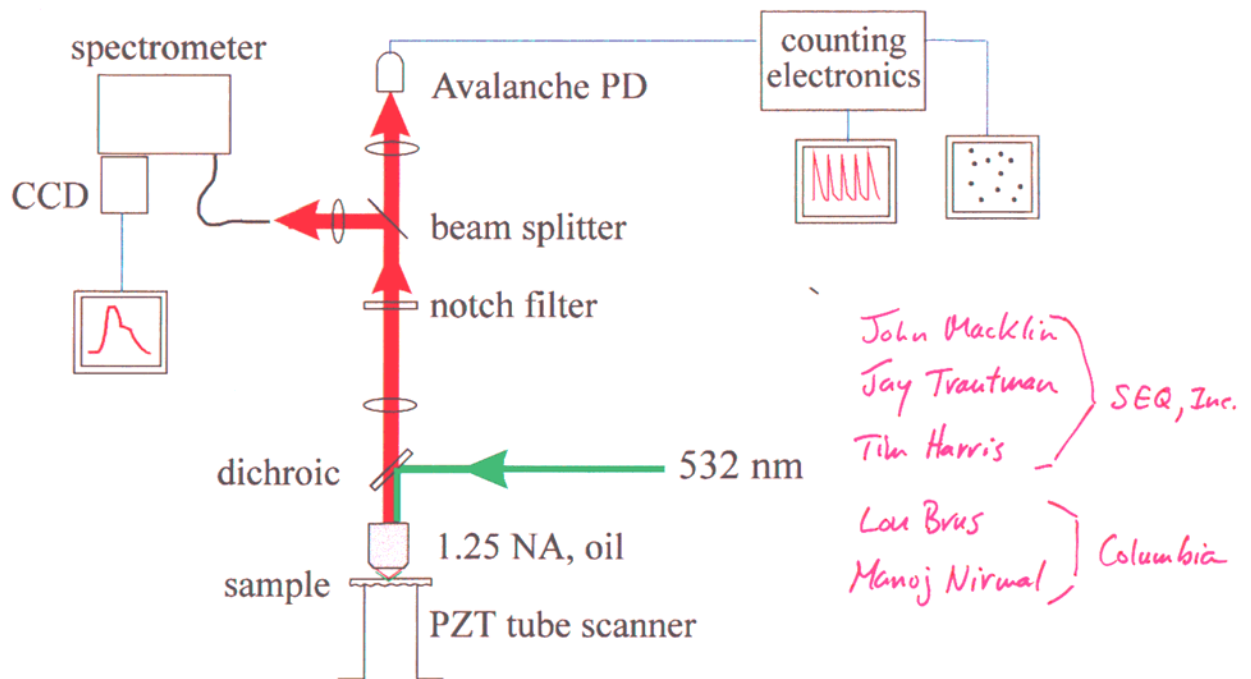
Betzig, Trautman (Bell Labs):
Confocal Scanned Stage Luminescence Spectrometer

Macklin etal, Science 272, 255 (1996)

Random Field of Single CdSe nanocrystals to cw optical excitation

a)

Raster scan image
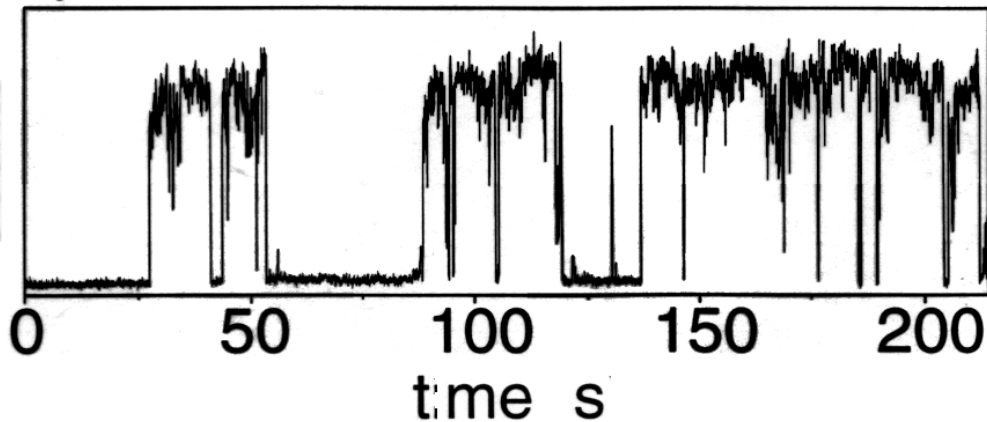
field of luminescing nanocrystals

Luminescence Image

1 um

Individual nanocrystals "blink" on and off

b)

Single Nanocrystal Luminescence
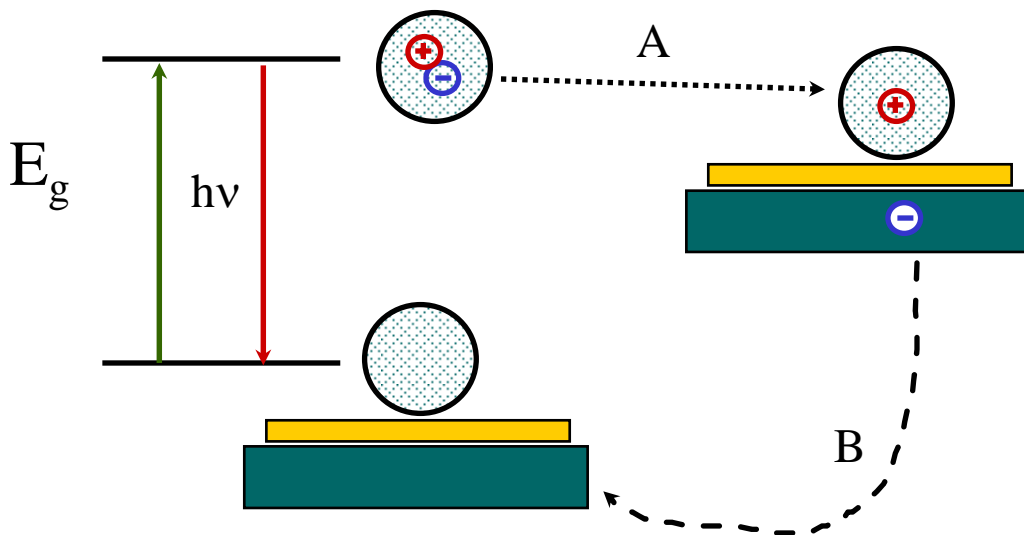
Counts

0   50   100   150   200

time s

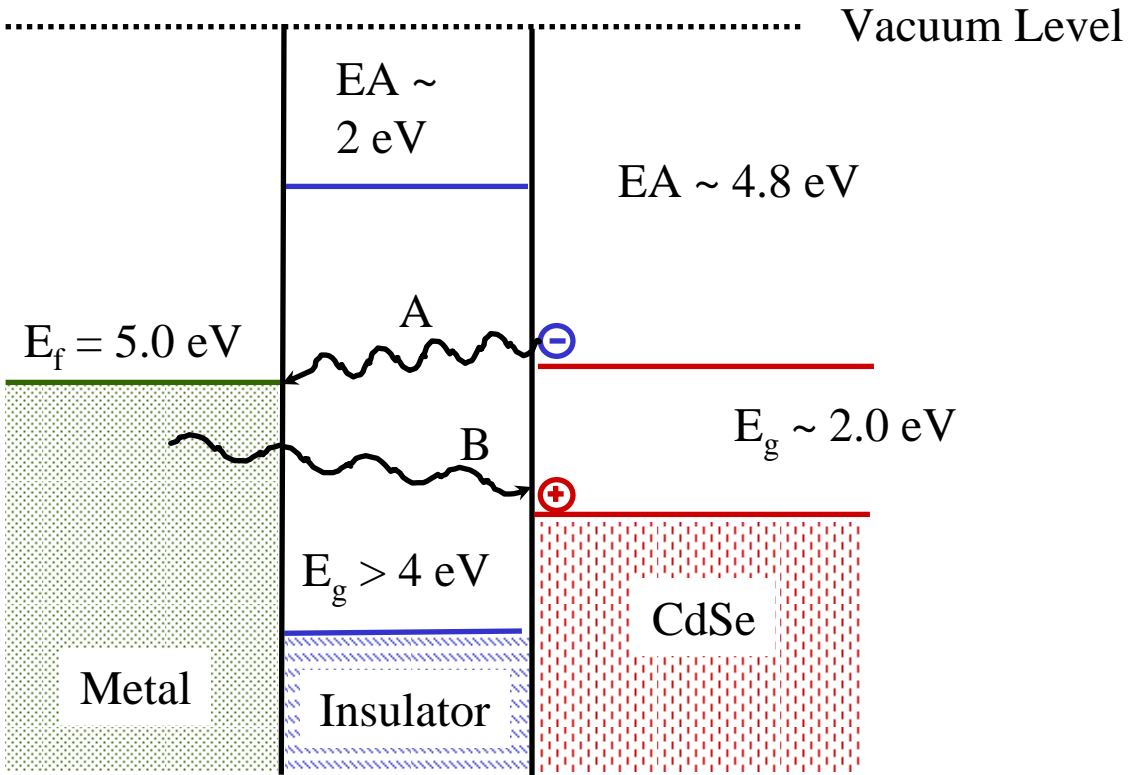Murwa etal Nature (accepted for publication

Nov 1996   Nature 383   2(66.   ig.

Nirmal etal, Nature 383, 802 (1996)

Schematic Blinking Mechanism: Photoionization and Re-neutralization

Vacuum Level

EA ~ 2 eV

EA ~ 4.8 eV

A

$E_f = 5.0$ eV

$E_g \sim 2.0$ eV

B

$E_g > 4$ eV

CdSe

Metal

Insulator

E_g

$h\nu$

A

B

Dark State: Ionized Nanocrystal with hole inside
Bright State: Neutral Nanocrystal

Direct Measurement of Electric Field Due to One Ionized Nanocrystal
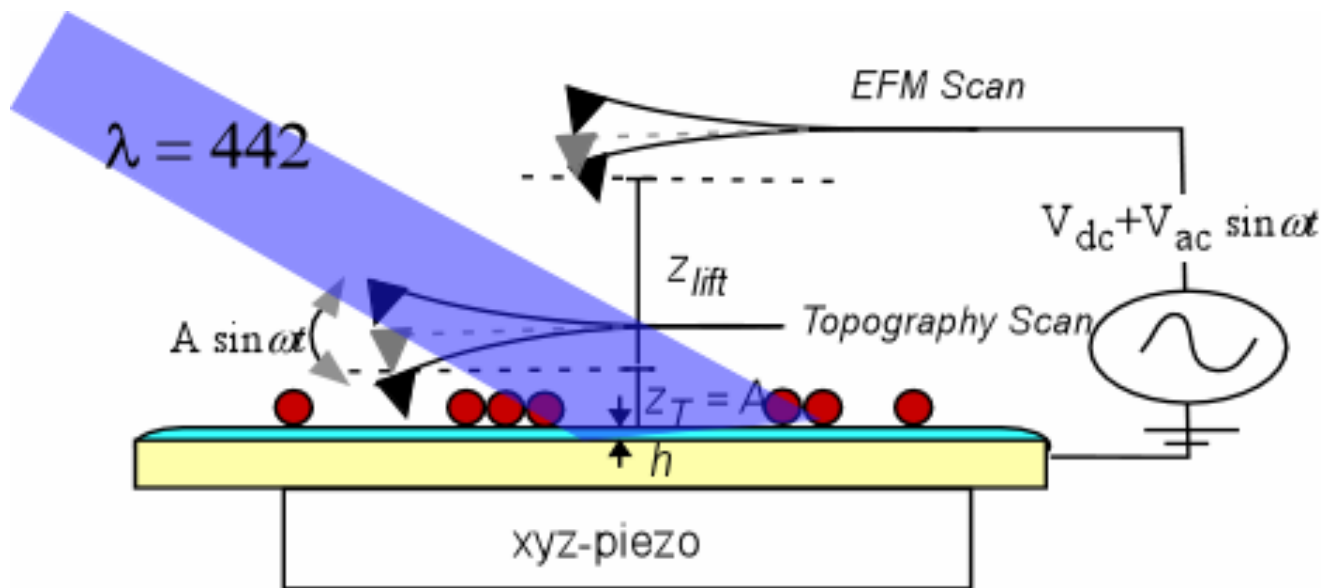
Electric Force Microscopy Invention:

Wickramasinghe IBM

Martin etal, Appl. Phys. Lett. 52, 1103 (1988)E

Can we measure a single charge on a single nanocrystal?

Electric Force Microscopy EFM

Oscillating Capacitor
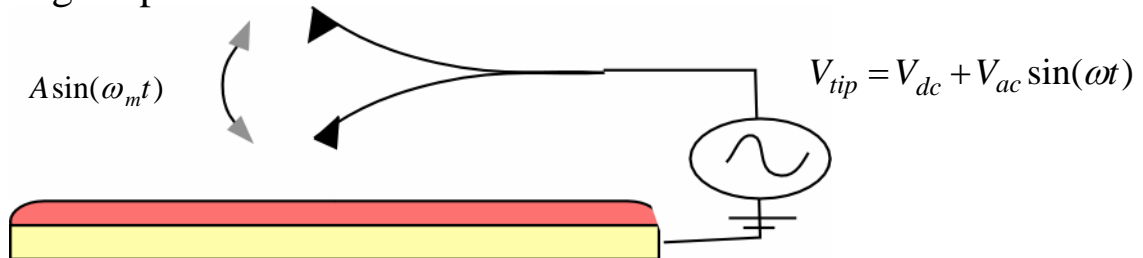
$A\sin(\omega_m t)$

$V_{tip} = V_{dc} + V_{ac}\sin(\omega t)$

Electrostatic Force $\qquad F_{coul} = \dfrac{Q_1 Q_2}{4\pi\varepsilon z^2}$

Energy Stored in a Capacitor $\qquad U = \dfrac{1}{2}CV^2 = \dfrac{1}{2}\dfrac{Q^2}{C}$

Capacitive Force $\qquad F = -\dfrac{dU}{dz} = -\dfrac{d}{dz}\left(\dfrac{1}{2}\dfrac{Q^2}{C}\right) = \dfrac{1}{2}\dfrac{Q^2}{C^2}\dfrac{dC}{dz} = \dfrac{1}{2}\dfrac{dC}{dz}V^2$

When a voltage is applied to the tip it feels a sum of electrostatic and capacitative forces. If there are static charges on the surface, image charges are induced in the metal tip.

$$F_e = F_{cap} + F_{coulomb} = \frac{1}{2}\frac{dC}{dz}V^2 + \frac{Q_1 Q_2}{4\pi\varepsilon z^2} \qquad\qquad V_{CPD} = (W_{substrate} - W_{tip})/(-e)$$

$$= \frac{1}{2}\frac{dC}{dz}\left((V_{dc} + V_{CPD}) + V_{ac}\sin(\omega t)\right)^2 - \frac{Q_s}{4\pi\varepsilon z}\left(Q_s + CV_{dc} + CV_{ac}\sin(\omega t)\right)$$

$$= \frac{1}{2}\frac{dC}{dz}\left((V_{dc} + V_{CPD})^2 + \frac{1}{2}V_{ac}^2\right) - \frac{Q_s}{4\pi\varepsilon z^2}\left(Q_s + C(V_{dc} + V_{CPD})\right)$$

$$+ \left(2(V_{dc} + V_{CPD})\frac{dC}{dz} - \frac{Q_s C}{4\pi\varepsilon z^2}\right)V_{ac}\sin(\omega t) + \frac{1}{4}\frac{dC}{dz}V_{ac}^2\cos(2\omega t)$$

$$\underbrace{\qquad\qquad\qquad\qquad}_{F(\omega)} \qquad \underbrace{\qquad\qquad}_{F(2\omega)}$$

CdSe/ZnS Charge Blinking on Graphite

Krauss etal J. Phys. Chem. 2001, B105, 1725

1ω   Charge image   2ω Polarizability image

← 400 nm →
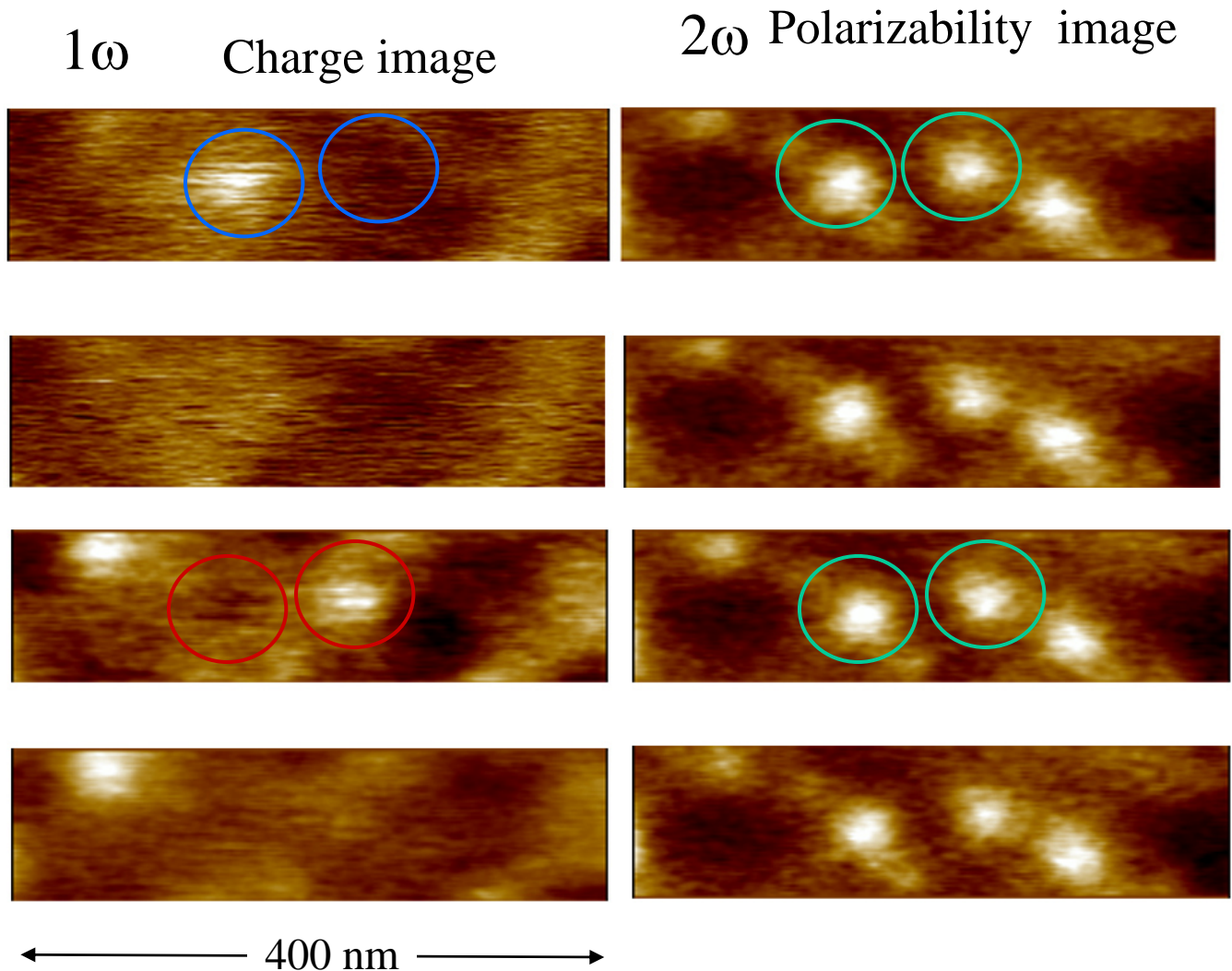
- Illuminated with 20 W/cm^2 at 442 nm

- Direct observation of Charge Blinking provides evidence for photoionization mechanism of Luminescence Blinking

Physical Size Regimes for Semiconductor Nanocrystals

Diameter, d (nm)	Atoms	Spectroscopic Regions		Kinetic Regions
				"solvent effect"
		Molecule		
0.7	10			Unimolecular e–h Kinetics
1.6	10^2			
3.4	10^3	Quantum Dot	← Bulk Exciton Diameter	
7.3	10^4			
15.6	10^5			
33.7	10^6	Shape Resonance		Band Bending
72.6	10^7	Polariton		Many-body Kinetics
156.0	10^8	$d=\lambda$ ↕ Size Resonance		
337.0	10^9			
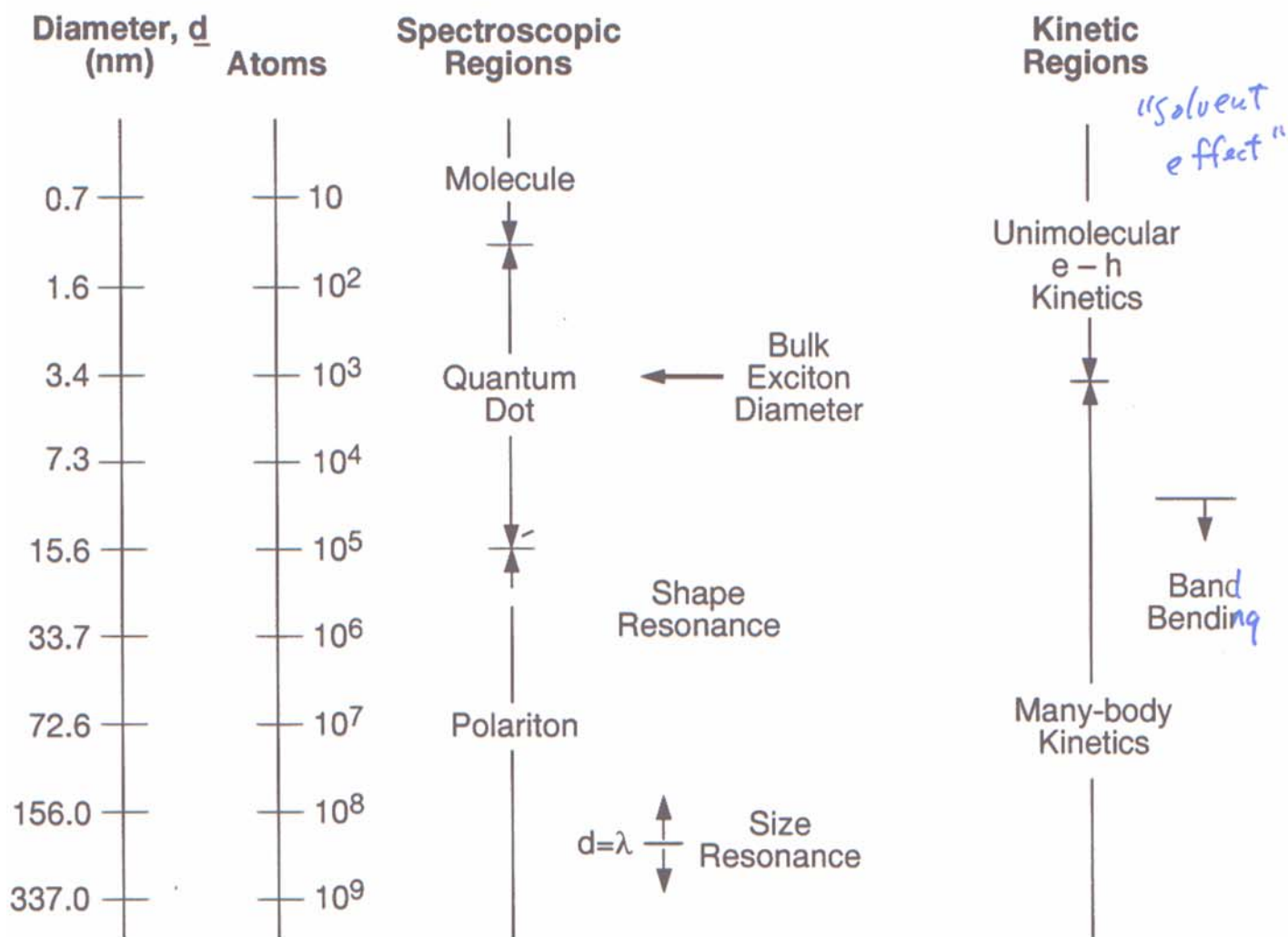
Evolution from molecules to solid state as size increases

MH4M20543.4